

AD-A115 279 CORNELL UNIV ITHACA NY
EQUATION OF STATE OF SIMPLE METALS.(U)
MAY 82 A L RUOFF, N W ASHCROFT

F/G 7/4

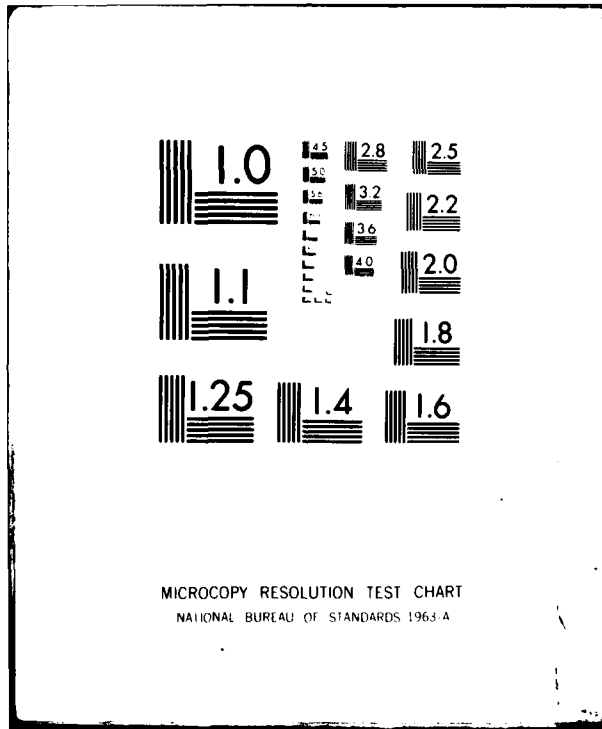
UNCLASSIFIED 8365-1

DAAG29-79-C-0188

ARO-14638.6-MS

NL

END
DATE
FILED
7 82
DTIC



ADA115279

UNCLASSIFIED

SECURITY CLASSIFICATION OF THIS PAGE (When Data Entered)

ARO 14638.6-MS

12

REPORT DOCUMENTATION PAGE		READ INSTRUCTIONS BEFORE COMPLETING FORM	
1. REPORT NUMBER 8365-1	2. GOVT ACCESSION NO. AD-A115 279	3. RECIPIENT'S CATALOG NUMBER	
4. TITLE (and Subtitle) EQUATION OF STATE OF SIMPLE METALS		5. TYPE OF REPORT & PERIOD COVERED Final 1/15/78 - 1/14/82	
		6. PERFORMING ORG. REPORT NUMBER DAAG29-79-C-0188	
7. AUTHOR(s) A. L. Ruoff and N. W. Ashcroft		8. CONTRACT OR GRANT NUMBER(s)	
9. PERFORMING ORGANIZATION NAME AND ADDRESS Cornell University, Ithaca, NY 14853		10. PROGRAM ELEMENT, PROJECT, TASK AREA & WORK UNIT NUMBERS	
11. CONTROLLING OFFICE NAME AND ADDRESS U. S. Army Research Office Post Office Box 12211 Research Triangle Park, NC 27709		12. REPORT DATE May 10, 1982	
13. MONITORING AGENCY NAME & ADDRESS (if different from Controlling Office)		14. NUMBER OF PAGES 13	
		15. SECURITY CLASS. (of this report) Unclassified	
		15a. DECLASSIFICATION/DOWNGRADING SCHEDULE	
16. DISTRIBUTION STATEMENT (of this Report) Approved for public release; distribution unlimited.			
17. DISTRIBUTION STATEMENT (of the abstract entered in Block 20, if different from Report) NA			
18. SUPPLEMENTARY NOTES The view, opinions, and/or findings contained in this report are those of the author(s) and should not be construed as an official Department of the Army position, policy, or decision, unless so designated by other documentation.			
19. KEY WORDS (Continue on reverse side if necessary and identify by block number) Equation of State, Potassium.			
20. ABSTRACT (Continue on reverse side if necessary and identify by block number) This is the final report of A. L. Ruoff and N. W. Ashcroft on the Equation of State of Simple Metals. It includes experimental equation of state results for potassium and theoretical calculations of its equation of state.			

DTIC FILE COPY

DD FORM 1 JAN 73 EDITION OF 1 NOV 65 IS OBSOLETE

UNCLASSIFIED

SECURITY CLASSIFICATION OF THIS PAGE (When Data Entered)

82 06 18 187

Report No. 8365-1

EQUATION OF STATE OF SIMPLE METALS

FINAL REPORT

A. L. RUOFF and N. W. ASHCROFT

MAY 10, 1982

U. S. ARMY RESEARCH OFFICE

CONTRACT DAAG29-79-C-0188

CORNELL UNIVERSITY

APPROVED FOR PUBLIC RELEASE:
DISTRIBUTION UNLIMITED.

TABLE OF CONTENTS

	<u>Page</u>
EXPERIMENTAL	1
THEORETICAL	7
I. Equilibrium and Transport Properties	7
II. Grüneisen Parameter & Dynamically Compressed Metals	9
III. Interatomic Forces in Transition Metals	10
IV. Electron Distributions Around Charge Centers in Solids	11



Accession For	
NTIS GRA&I	<input checked="" type="checkbox"/>
DTIC TAB	<input type="checkbox"/>
Unannounced	<input type="checkbox"/>
Justification	
By _____	
Distribution/ _____	
Availability Codes	
Dist	Avail and/or Special
A	

EXPERIMENTAL

Precision measurements of volume versus pressure for one meter long potassium specimens have been successfully carried out up to a hydrostatic pressure of 7 kbar. The length change of the specimen has been measured to an accuracy of better than 500 Å using a He-Ne laser interferometer in a temperature controlled environment with temperature variations $\pm 0.001^{\circ}\text{C}$ at 28.58°C .

Extensive work was required to grow these large single crystals of a reactive material and considerable work was needed to develop techniques for handling these large, reactive, compliant and weak crystals. The successful growth of this crystal can only be described as a tour de force. It took us much longer than expected because it was much harder than expected.

Potassium immersed in a mineral oil environment inside a 5 gallon pail was purchased from Mine Safety Appliance Corporation, Evans City, PA, with a 99.95% purity. It was transferred from the 5 gallon pail into an extrusion vessel specially made for handling potassium. Since potassium, like other alkali metals, is very soft and oxidizes rapidly in moisture and air, transfer was made directly into the extrusion vessel filled with liquid hexane which had been previously purified and dehydrated by keeping it in the container with a large amount of potassium chips under slight pressure of ultra high purity argon gas. Then the extrusion was carried out into a pyrex glass tube which was also filled with pre-purified liquid hexane to a desired length (about 130 cm long) using a 7.9 mm die. This extruded potassium was zone-refined several times to enhance purity and anneal-out defects and some of the dislocations. It was then finally transferred to our length measurement pressure vessel. Liquid hexane, purified as described above, was used as a pressurizing medium.

Our data have been analyzed by a special non-linear least square fit of various equations of state to obtain the isothermal bulk modulus and its pressure derivatives at atmospheric pressure.

The first order Murnaghan equation (ME_1) which assumes that all pressure derivatives of the bulk modulus at zero pressure beyond the first are zero, the second order Murnaghan equation (ME_2), two parameter Birch equation (BE_1), three parameter Birch equation (BE_2), and Keene equation yield the following results listed in Table I below.

Table I. Bulk modulus and its pressure derivatives for potassium at 28.58°C.

Equation Used	B_0 (kbar)	B_0'	B_0'' (kbar) $^{-1}$
ME_1	31.01 ± 0.02	3.905 ± 0.009	
ME_2	30.87 ± 0.01	4.094 ± 0.018	-0.0747 ± 0.0068
BE_1	30.85 ± 0.01	4.144 ± 0.003	-0.131 ± 0.002
BE_2	30.85 ± 0.02	4.151 ± 0.021	-0.135 ± 0.01
KE	30.84 ± 0.02	4.159 ± 0.024	-0.145 ± 0.014

In the above table, B_0 , B_0' and B_0'' are the values of bulk modulus, its first pressure derivative, and its second pressure derivative, taken at atmospheric pressure, respectively. The above data are to be compared with Swenson's values [C. E. Monfort and C. A. Swenson, J. Phys. Chem. Solids 26, 291 (1965)] obtained by the piston-cylinder method and Smith's ultrasonic measurements [P. A. Smith and C. B. Smith, J. Phys. Chem. Solids 26, 279 (1965)]. Their data were fitted by ME_1 which is based on the assumption that $B = B_0 + B_0'P$, and yield

$$B(\text{kbars}) = 30.8 + 3.85 P \quad (\text{Swenson})$$

$$B(\text{kbars}) = 30.9 + 3.98 P \quad (\text{Smith})$$

The manner of fitting is itself very important; note how B_0' of our data changes when ME_2 is used rather than ME_1 . Thus Swenson's B_0' would be increased from 3.85 if ME_2 or other higher order equations were used. It is quite exciting to see that our values for B_0 are in excellent agreement with those obtained by Swenson and Smith and that the B_0' values are close. It should be noted that various theories of binding show that the Maclaurin series for $B(P)$ involves alternating signs for the derivatives, with B_0' positive, B_0'' negative, etc. Hence the use of ME_1 will give a lower bound on B_0' and an upper bound on B_0 , because of the neglect of the negative $B_0''P^2/2$ term. Similarly, the use of ME_2 should give a lower bound on $|B_0''|$, an upper bound on B_0' and a lower bound on B_0 . Thus we can expect from our results alone: $30.86 \leq B_0 \leq 31.03$ and $3.90 \leq B_0' \leq 4.11$. These results have been published.

The second pressure derivative of the bulk modulus, B_0'' , exhibits some dispersion and uncertainty around the value of $-0.1(\text{kbar})^{-1}$, depending on the equation of state used, as shown in Table I. This is expected from the fact that B_0'' involves a third derivative taken from the pressure-volume data. The meaningful determination of B_0'' requires not only an extremely accurate volume measurement with an error $\Delta V/V_0 \lesssim 10^{-6}$, as pointed out by Macdonald and Powell [J. R. Macdonald and D. R. Powell, J. Res. NBS 25A, 441 (1971)], but also an equal accuracy in the pressure measurements, as indicated by Kim, Chhabildas and Ruoff [K. Y. Kim, L. C. Chhabildas and A. L. Ruoff, J. Appl. Phys. 47, 2862 (1976)]. The former condition is certainly fulfilled in our volume measurement, but the latter is extremely difficult to meet in the laboratory.

The Grover, Getting, Kennedy equation [R. Grover, I. C. Getting and G. C. Kennedy, Phys. Rev. 7, B 567 (1973)] has been proposed as a two parameter equation involving B_0 and B_0' . Higher derivatives of the bulk modulus are not zero but can be directly determined from B_0 and B_0' ; we find

$$B_0'' = - \frac{B_0'^2}{B_0} , \quad (GGK)$$

which gives $B_0'' \approx -0.54$. This is too large by a factor of four to seven; thus GGK is incorrect on a physical basis (just as ME₁ is); nonetheless both equations have some practical use.

Instead of trying to meet the latter condition, the accuracy of B_0'' can be improved, as far as pressure is concerned by extending the applied pressure range up to pressure equal to B_0 (kbars) of a specimen or even beyond. A potassium crystal has $B_0 \approx 30$ kbar. A 30 kbar vessel was constructed to carry our length measurements out to this pressure.

The overall view of a 30 kbar vessel is displayed in Figure 1. The two stage pressure vessel design has been adopted to generate a maximum pressure of 30 kbar in the bore of the inner vessel. These vessels were made of a non-magnetic titanium alloy, the product of Reactive Metal Corporation, RMI 38-6-44. The commonly used manganin wire pressure sensor and a new type of pressure sensor built with a chip size stable Zener diode have been constructed and were tested in order to accurately calibrate and measure pressure up to 30 kbar. Improved feed-through of the electrical leads into 30 kbar vessel has been devised to electrically detect the change under pressure.

Unfortunately, the contract was not renewed and came to an end just as the vessel was being installed and tested.

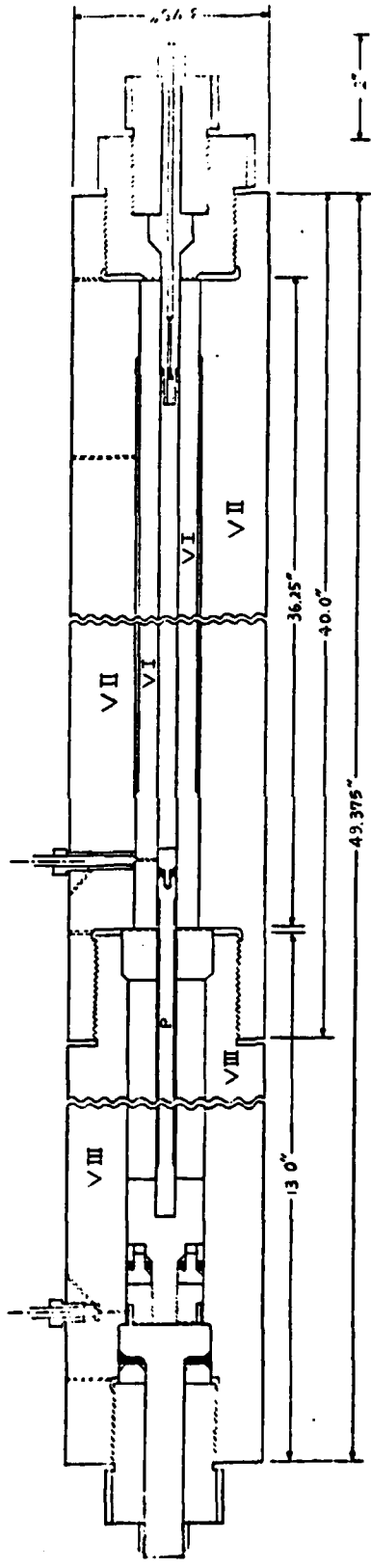


Figure 1. Overall view of 30 kbar pressure system.
VI. inside pressure vessel; VII. outside supporting pressure vessel;
VIII. intensifier pressure vessel; P. piston.

Publication

1. K. Y. Kim and A. L. Ruoff, "Isothermal Equations of State of Potassium",
J. Appl. Phys. 52, 245 (1981).

THEORETICAL

I: Equilibrium and Transport Properties

The major emphasis of the early part of the theoretical program centered on the equation of state and transport properties of both potassium and aluminum. The objective of the program had been to study the suitability of the simple metals as possible monitors of pressure in ultra-pressure environments. Under such conditions it is likely that resistivity can be measured, and for this reason we concentrated our attention on electrical transport properties. These are usually calculated as functions of volume, whereas the quantity of most practical significance is the resistivity (or resistance) as a function of pressure. It is therefore necessary to know the equation of state of the metal, particularly under conditions of high compression. As described in the original proposal, we pursued this aim on a metal with relatively low bulk modulus; potassium has a zero pressure bulk modulus B_0 of 30 Kbar and we examined the theoretical equation of state at pressures far in excess of 30 Kbar. The ability of the current theory of the metallic state to describe the equation of state of a metal for pressure greater than B_0 in a soft metal (such as potassium) was taken as evidence that the same theory would be successful in describing a simple metal, such as aluminum, with a much higher bulk modulus.

These two metals do differ, however, in an important respect. The ions of aluminum are compact and very tightly bound. In comparison, the ions of potassium are more extended and less tightly bound electronically. As a

consequence, core-polarization effects in potassium cannot be neglected in an accurate determination of the equation of state. Thus in our detailed study (1) we re-examined the theory of the ground state energy of simple metals and included the electron-electron interaction effects between localized core-states. This meant modifying the method of structural expansions (2,3) to include the effects of core-polarization fluctuations. It is well known that in insulating systems such fluctuations lead to Van der Waals interactions at long range. In a metal, however, these interactions are screened by the valence electrons, and since the processes involved are dynamic, the screening requires a knowledge of the frequency dependent dielectric function of the interaction electron gas. That even the screened Van der Waals interactions in potassium are appreciable at high pressures can be attributed to the fact that the polarizability of the potassium ion is rather substantial. The results (1,4) showed that although it is reasonable to ignore core-polarization at low pressure ($P < 10$ Kbar) they become progressively more important at higher pressures; for example, they contribute about 15 Kbar (out of approximately 60) at 40% compression (5).

In addition to the question of the equation of state we also examined quite closely the behavior of the high temperature resistivity of aluminum under pressure (6). To minimize errors as much as possible, we considered the scaled resistivity, i.e., $\rho(P)/\rho(P=0)$, by determining ρ from a standard variational treatment of the Boltzmann equation in which the necessary electron levels and distortion of the actual Fermi surface were obtained from a replicated two plane-wave model. The scaled resistivity that resulted displayed a very clear minimum (6) at a pressure of about 25 GPa. We were able to understand this behavior in terms of the increasing importance of

distortions to the Fermi surface as pressure itself increased. In this respect, the results for the crystal are very different from those we obtained (7) for liquid aluminum which possesses a spherical Fermi surface. And since the distortions to the Fermi surface in the crystal reflect the changes in pseudopotential with density, the behavior among different crystalline simple metals is also quite varied (we predict lead to have a $\rho(P)$ rather different from that found in Al).

II: Grüneisen Parameter and Dynamically Compressed Metals

A major part of the theory component concerned the direct study of the Grüneisen parameter, the quantity required in reducing the shock data to isothermal conditions. To obtain this quantity with precision we required, as functions of temperature and volume, the bulk modulus, the heat capacity, and the coefficient of volume expansion.

As described above we made some advances in understanding the equation of state of potassium at high density, our major interest was directed toward the $T = 0$ isotherm. Subsequently we examined the contribution of the phonons to the free energy of a model solid using the method of self-consistent phonon theory (7). This approach allows us to build in the effects of the most important anharmonicities, and while these are reasonably small effects at low temperatures, they become increasingly important at high temperatures (for instance, in the conditions prevailing in shock experiments). Another method we developed (and are currently improving) gives a different approach to the problem. In this new method (9) the thermodynamic properties of simple solids at high pressures are calculated from liquid state thermodynamics by treating the solid as a super-cooled liquid. In particular,

we are able to obtain the energy and pressure at arbitrary temperatures and densities via expressions that are reasonably simple functionals of the pair potential. As an application of this principle, we have started to analyze shock-wave data via liquid state thermodynamics. For example, we can use shock-wave data directly as a test of a given pair potential without resorting to the usual techniques for "reduction of the Hugoniot." Alternatively, the method can be used to perform the reduction of a shock Hugoniot by selecting from a general space of pair potentials the one that best fits the known equilibrium thermodynamic quantities and the Hugoniot curve. The resulting pair interaction can subsequently be used to generate zero temperature data thereby also performing a "reduction."

III: Interatomic Forces in Transition Metals

We extended our early work supported by the grant on simple metals to transition metals to the extent that their electronic structure could be reasonably well described by the tight binding approximation. In particular, we derived a new method (10) for calculating the interatomic potentials that can be attributed to band broadening contributions to the metallic cohesive energy. Our method was based on the direct evaluation in r-space of the moments of the electronic density of states, but projected on a particular atom. We applied it to tight-binding model Hamiltonians appropriate to either one- or five-states per atom. In the latter case, which is appropriate to the d-orbitals in transition metals, the resulting interatomic potentials have spatial forms rather characteristic of fluctuating multipole forces. The band broadening contributions are attractive: the expected short-range repulsive contributions are obtained by expanding the energy

to second order in atomic orbital overlaps. The combination of attractive and repulsive contributions forms the basis of our method for calculating the thermodynamic functions in the transition metals and parallels the nearly free electron approach we used in the simple metals. So far, we have applied the method to the study of vacancy formation energies.

IV: Electron Distributions Around Charge Centers in Solids

Finally, in the course of studying pair and multi-center interactions in solids, we were led to consider the nature of electron distributions around point charges in many-body systems. We managed to prove a cusp theorem (11) which relates the zero-separation value and slope of two-particle positional correlation functions in quantum many-body systems with Coulombic interactions. The theorem is independent of particle type and symmetry of the wave-function. Our proof uses only the integral form of the Schrödinger equation and continuity and long-range exponential decay of the wave function. We have used the theorem to derive a sum-rule for the electron gas structure factor, and an exact statement about the screening of point charges.

Partial References

1. J. Cheung, "Structural and Transport Properties of Simple Metals under High Pressure," Thesis, Cornell University, 1979.
2. N. W. Ashcroft and D. C. Langreth, "Compressibility and Binding Energy of Simple Metals," Phys. Rev. 155, 682 (1967).
3. J. Hammerberg and N. W. Ashcroft, "Ground State Energies of Simple Metals," Phys. Rev. B9, 409 (1974).
4. J. Cheung and N. W. Ashcroft, "Screened Polarization Waves and the Energies of Simple Metals: Formulation," Phys. Rev. B23, 2484 (1981).
5. J. Cheung and N. W. Ashcroft, "Core Polarization and the Equation of State of Potassium," Phys. Rev. B24, 1636 (1981).
6. J. Cheung and N. W. Ashcroft, "Aluminum under Pressure. II. Resistivity," Phys. Rev. B20, 2991 (1979).
7. J. Cheung and N. W. Ashcroft, "Resistivity of Liquid Metals under Elevated Pressure," Phys. Rev. B18, 559 (1978).
8. See, for example, D. Stroud and N. W. Ashcroft, "Theory of Melting of Simple Metals: Application to Na," Phys. Rev. B5, 371 (1972).
9. R. S. Jones and N. W. Ashcroft, "Analysis of Shock Wave Data via Liquid State Thermodynamics" (to be published).
10. A. Carlsson and N. W. Ashcroft, "Pair Potentials from Band Theory: Application to Vacancy Formation Energies" (to be published).
11. A. Carlsson and N. W. Ashcroft, "Asymptotic Freedom in Solids: A Theorem," Phys. Rev. B25, XXXX (1982).

Publications

1. J. Cheung and N. W. Ashcroft, "Aluminum under High Pressure.
II. Resistivity", Phys. Rev. B 20, 2991 (1979).
2. J. Cheung and N. W. Ashcroft, "Core Polarization and the Equation of
State of Potassium", Phys. Rev. B 24, 1636 (1981).

Isothermal equations of state of potassium

Kwang Yul Kim and Arthur L. Ruoff

Department of Materials Science and Engineering, Cornell University, Ithaca, New York 14853

(Received 21 July 1980; accepted for publication 30 September 1980)

Volume versus pressure data of 1-m-long polycrystalline potassium has been obtained as a function of hydrostatic pressure up to 7 kbars at 28.58 °C. The length change has been measured to an accuracy of less than 500 Å using a Fabry-Perot type He-Ne laser interferometer in a temperature-controlled environment with temperature variations ± 0.001 °C. The isothermal bulk modulus B_0 and its pressure derivative B'_0 at atmospheric pressure and 28.58 °C are $B_0 = 31.01 \pm 0.02$ kbars and $B'_0 = 3.91 \pm 0.01$, when the first-order Murnaghan equation is used; and $B_0 = 30.84 \pm 0.02$ kbars and $B'_0 = 4.16 \pm 0.02$, when the Keane equation is used. The Keane equation yields $B''_0 = -0.145$ kbar⁻¹ in the applied pressure range. Various two- and three-parameter equations of state have been used to fit the measured pressure-volume data. The Keane and Birch equations represent the data most closely when these equations are extrapolated into a higher-pressure region.

PACS numbers: 64.30. + t, 64.10. + h, 62.50. + p

INTRODUCTION

Potassium and the other alkali metals have drawn considerable theoretical interest. The measurement of their thermodynamic properties is helpful in understanding the cohesion of simple metals. However, their mechanical softness and strong chemical reactivity have made these measurements very unattractive, since extreme care must be taken in handling these materials.

Earlier measurements of volume compression of alkali metals were carried out by Bridgeman¹⁻⁴ up to 100 kbars. The pressure scale he used in a higher-pressure region turned out to deviate appreciably from the present pressure scale. Swenson and his coworkers^{5,6} measured volume change up to 20 kbars over a temperature range down to liquid-helium temperature. Kennedy and his collaborators⁷ have measured the pressure-volume isotherms up to 45 kbars. Both of the above authors used the piston-cylinder device. But the quasi-hydrostatic media and corrections due to the piston compression and friction contribute to errors in their measurements. Our present measurements are under purely hydrostatic conditions.

Let V denote the volume of a specimen under pressure P and at some constant temperature T . Then an isothermal bulk modulus B is defined and expanded in terms of pressure as

$$B = -V \left(\frac{\partial V}{\partial P} \right)_T \\ = B_0 + B'_0(P - P_0) + \frac{1}{2} B''_0(P - P_0)^2 + \dots \quad (1)$$

where

$$B_0 = V_0 \left(\frac{\partial V}{\partial P} \right)_{T, P_0}, \quad B'_0 = \left(\frac{\partial B}{\partial P} \right)_{T, P_0},$$

and

$$B''_0 = \left(\frac{\partial^2 B}{\partial P^2} \right)_{T, P_0}$$

are evaluated at atmospheric pressure P_0 .

Although most of those measurements made by the above workers are quite adequate to describe thermodynamic behaviors at high pressures, they are not precise enough to derive reliable higher-order pressure derivatives of bulk modulus, such as B''_0 or higher. The potassium crystal is an extremely soft solid with $B_0 \approx 30$ kbars and B''_0 is expected to contribute appreciably to the value of B at higher pressures.

Accurate measurements of adiabatic bulk modulus by the ultrasonic method have been made by Smith and his coworkers.⁸ The ultrasonic method yields adiabatic data which, if isothermal results are desired, must be converted by resorting to Overton's relation.⁹ The Overton formulas involve a number of parameters, all of which are not accurately determined in the desired pressure range.

Given our precise length change measurements with resolution better than 500 Å for a 1-m-long potassium specimen, B_0 , B'_0 , and B''_0 have been determined by statistically fitting the data to several isothermal equations of state. A detailed treatment and discriminations between these equations have been described by Macdonald and his coworkers.^{10,11} Macdonald and Powell¹¹ have shown that it is statistically insignificant to discriminate the equations of state in a

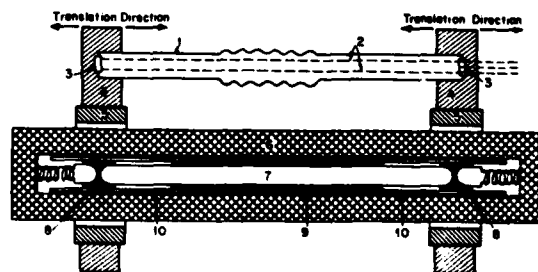


FIG. 1. Schematic of length measurement system. 1: laser path vacuum bellows, 2: laser beam, 3: interferometer mirrors, 4: coupling plates, 5: LVDT's, 6: pressure vessel, 7: specimen, 8: magnetic cores, 9: stainless-steel tube, 10: Pyrex glass tube.

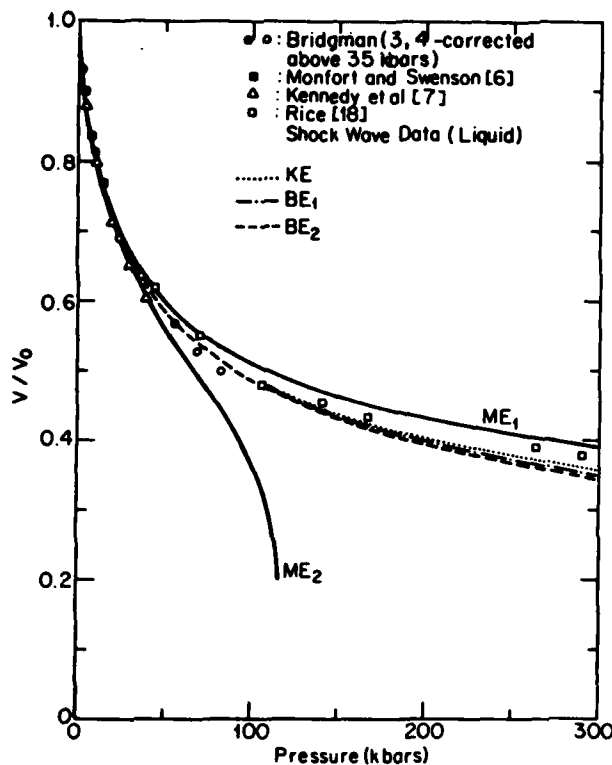


FIG. 2. Extrapolation of pressure-volume data for potassium. Bridgman's pressure scale correction above 35 kbars, 40→38 kbars, 60→56 kbars, 80→70 kbars, and 100→84 kbars. The shock data are for liquid metal.

low-pressure region ($P/B_0 < 0.01$) unless the experimental data are very accurate within an error of $\Delta V/V_0 < 10^{-6}$. The precision in our length change measurement is better than 5×10^{-8} and $P/B_0 < 0.25$.

EXPERIMENTAL METHOD

A detailed description of the experimental setup has been provided by Lincoln and Ruoff.¹² As shown in Fig. 1, a polycrystalline potassium rod which is approximately 1 m

long and 7.9 mm in diameter was inserted in a tube, which in turn is held inside the 12.7-mm-diam bore of the nonmagnetic titanium alloy pressure vessel. The central portion of the tube is 304 stainless steel and the remaining part of the tube, where the magnetic cores of the linear variable differential transformer (LVDT) are slightly spring-loaded against both ends of the potassium specimen, is a Pyrex glass tube which is used to avoid any spurious magnetic effects on the H-shaped magnetic cores.

Potassium was obtained from Mine Safety Appliance Corporation and is 99.95% pure. This was extruded into a 7.9-mm die to the desired length. It is then zone refined several times to enhance purity and to anneal out defects and some dislocations. A more elaborate ball bushing arrangement for holding the specimen to minimize friction was previously used.¹²⁻¹⁴ This was not adopted in this experiment, because the small difference in density between potassium and the pressurizing medium (liquid hexane) keeps friction sufficiently small. Dehydrated liquid hexane is used as the pressure fluid. Pressure was measured by using a manganin wire pressure sensor. The calibrating technique of the manganin gauge is described in detail elsewhere.¹⁵

The length measurements were made at an interval of 300 bars up to a maximum pressure of 7 kbars. Inasmuch as the linear compressibility of polycrystalline potassium is isotropic, volume measurements are obtained, using the relation $V/V_0 = (l/l_0)^3$. Resolution in the length measurements of the He-Ne laser interferometry is better than 300 Å in the temperature stabilized environment with thermal noise of 0.001 °C.

The LVDT electronics, laser interferometer, coupling plates and their translation motion, and temperature control, etc., have been described in detail in the literature.¹²

DATA ANALYSIS

For notational convenience, we shall introduce the following abbreviations: $p = P - P_0$, $\eta = B_0'$, $\psi = B_0 B_0''$, $z = P/B_0$, and $x = V_0/V$. Note that η , ψ , z , and x are all dimensionless quantities. P_0 is assumed to be 1 bar in this

TABLE I. Various equations of state.

Equation	Acronym	Form
First-order Murnaghan	ME ₁	$z = \eta^{-1}(x^4 - 1)$
Second-order Murnaghan	ME ₂ ($\eta^2 > 2\psi$)	$z = 2(x(\eta^2 - 2\psi)^{1/2} - 1)/[(\eta^2 - 2\psi)^{1/2}]$ $\times (x(\eta^2 - 2\psi)^{1/2} + 1) - \eta(x(\eta^2 - 2\psi)^{1/2} - 1)]$
Keane	KE ($-\eta^2 < \psi < 0$)	$z = [\eta^3/(1 - \eta^2 + \psi^2)]$ $\times (x^{1/2} + \psi/x - 1) - [\psi/(\eta^2 + \psi)] \ln x$
First-order Birch	BE ₁	$z = \frac{3}{2}(x^{7/3} - x^{5/3})(1 + \frac{3}{2}(\eta - 4)(x^{2/3} - 1))$
Second-order Birch	BE ₂	$z = \frac{3}{2}[x^{7/3} - x^{5/3}](1 + \frac{3}{2}(\eta - 4)(x^{2/3} - 1))$ $+ \frac{1}{2}\{143 + 9\eta(\eta - 7) + 9\psi\}(x^{2/3} - 1)^2]$
Grover Getting, Kennedy	OGKE	$B_T = B_0^T \exp[\eta(1 - x^{-1})]$

TABLE II. Bulk modulus and its pressure derivatives for potassium at 28.58 °C.

Equation Used	B_0 (kbar)	B'_0	B''_0 (kbar $^{-1}$)
ME ₁	31.01 ± 0.02	3.905 ± 0.009	0
ME ₂	30.87 ± 0.01	4.094 ± 0.018	-0.0747 ± 0.0068
GGKE	30.81 ± 0.01	4.184 ± 0.004	-0.568 ± 0.001
BE ₁	30.85 ± 0.01	4.144 ± 0.003	-0.131 ± 0.002
BE ₂	30.85 ± 0.02	4.151 ± 0.021	-0.135 ± 0.010
KE	30.84 ± 0.02	4.159 ± 0.024	-0.145 ± 0.014

*Obtained from B_0 and B'_0 .

paper. Several of the two- and three-parameter phenomenological equations described in detail elsewhere^{10,16} are used to fit the pressure-volume data and are listed in Table I.

Table II shows the values of the bulk modulus and its pressure derivatives obtained by fitting the measured pressure volume data into the equations of state listed in Table I. ME₁ is the only equation of state in the list for which B''_0 is zero. The expressions for BE₁ and GGKE do not explicitly contain the parameter B''_0 ; however, this does not imply that B''_0 is identically zero. The appropriate expression for B''_0 in the case of BE₁ can be obtained by setting the third term in the second-order Birch equation BE₂ equal to zero. The result is

$$9B_0B''_0 = -[143 + 9B'_0(B'_0 - 7)]. \quad (2)$$

Successively differentiating the GGKE equation with respect to pressure and taking the limit as $P \rightarrow P_0$, one obtains

$$B_0B''_0 = -B'^2. \quad (3)$$

GGKE, along with several other equations of state, fits the pressure-volume data well. However, a low value of B'_0 (30.8 kbars) gives an unreasonably high value of B''_0 , as expected from Eq. (3).

Another approach for the determination of the bulk modulus at each pressure point is to combine three neighboring data points and fit them into ME₁. That is,

$$\int_{V_1}^{V_2} \frac{dV}{V} = \int_{P_1}^{P_2} \frac{dP}{B_0 + B'_0(P - P_1)}, \quad (4)$$

$$\int_{V_1}^{V_2} \frac{dV}{V} = \int_{P_1}^{P_2} \frac{dP}{B_0 + B'_0(P - P_1)}. \quad (5)$$

Out of the two relations (4) and (5), B_0 and B'_0 have been numerically calculated at each pressure point (except $P = P_0$ and $P = P_{max}$). These bulk modulus versus pressure data are statistically fitted, using the formula

$$B = B_0 + \sum_{n=1}^N \frac{1}{n!} B_0^{(n)} (P - P_0)^n, \quad (6)$$

where

$$B_0^{(n)} = \left(\frac{\partial^n B}{\partial P^n} \right)_{P=P_0}. \quad (7)$$

The values of B_0 and $B_0^{(n)}$ for $N = 1, 2$, and 3 are displayed in Table III.

As expected, ME₁ in Table II and $N = 1$ in Table III, yield essentially the same result for B_0 and B'_0 , and ME₂ in Table II and $N = 2$ in Table III also show essentially the same result for B_0 , B'_0 , and B''_0 , within experimental errors, respectively. This provides a self-consistency check for ME₁ and ME₂. It is interesting to notice that $N = 3$ in Table III provides almost identical results for B_0 , B'_0 , and B''_0 to those which BE₂ and KE yield (Table II). Note that the neglect of B''_0 in ME₁ leads to a B'_0 value which is too small.

Table IV shows the data of bulk modulus and its pressure derivatives measured by other authors together with the present work for the sake of comparison. The agreement in B'_0 is only adequate when compared with Bridgman and Kennedy's static compression data, but B_0 and B'_0 are in good agreement with Swenson's static compression data and Smith's values obtained by the ultrasonic technique.

DISCUSSION

As can be seen in Tables II and IV, the two- and three-parameters equations yield virtually identical results for B_0 , and values of B'_0 obtained from GGKE, BE₁, BE₂, and KE are also in good agreement. Although any sign of curvature is hardly noticeable in the ultrasonic measurements of $B(P)$ vs P for potassium,⁹ the three-parameter equations (ME₂, BE₂, KE) show unmistakably a negative value of $B''_0 \approx -0.1$ kbar $^{-1}$. Anderson¹⁷ used Swenson's value^{5,6} for B_0 and B'_0

TABLE III. Values of B_0 and $B_0^{(n)}$ for $N = 1, 2$, and 3 .

N	B_0 (kbar)	B'_0	B''_0 (kbar $^{-1}$)	B'''_0 (kbar $^{-2}$)
1	31.06 ± 0.05	3.88 ± 0.02	0	0
2	30.86 ± 0.04	4.09 ± 0.03	-0.073 ± 0.010	0
3*	30.81 ± 0.05	4.18 ± 0.08	-0.145 ± 0.063	0.024 ± 0.021

*Because of the large standard deviation associated with B''_0 and the much larger standard deviation associated with B'''_0 than with the $N = 2$ case, the numbers in this row should not be given great significance.

TABLE IV. Isothermal bulk modulus and its pressure derivatives of potassium (equation used: ME₁, ME₂, ME₃).

Source	Temperature (°C)	B_0 (kbar)	B'_0	B''_0 (kbar ⁻¹)	B'''_0 (kbar ⁻²)
Bridgman ⁴	Room	33.25	3.43		
Swenson ⁵	25°	30.8	3.85		
Smith ⁶	Room	30.9	3.98		
Kennedy ⁷	Room	34.0	2.99		
This work ^b	28.58	31.2	3.65	-0.039	
	28.58	30.87	4.09	-0.075	
	28.58	30.81	4.18	-0.145	0.024

^aCorrected to an isothermal value from ultrasonic data.^bSee comment in Table III regarding last row of data.

taken at low pressures on the solid and chose B''_0 which can best fit the shock wave data¹⁸ (which is for the liquid) taken at higher pressures, using the Keane equation. He obtained the values of $B''_0 = -0.051 \text{ kbar}^{-1}$ for potassium and $B''_0 = -0.031 \text{ kbar}^{-1}$ for sodium. Similar procedures have been used by Fritz and Thurston¹⁹ by using a different type of extrapolation formula. Their values of B''_0 are -0.018 kbar^{-1} for potassium and 0.024 kbar^{-1} for sodium. Considering that this involves mixing shock data on the liquid with low-pressure isothermal data on the solids, these values of B''_0 should not be taken seriously.

The value of B''_0 shows very sensitive dependence not only on the accuracy of the V/V_0 measurement, as pointed out by MacDonald and Powell,¹¹ but also on the functional form of the variation of pressure with the change in resistance per unit resistance $\Delta R/R_0$ of the manganin gauge, as indicated in the data of LiF and NaCl.^{13,14} Our pressure measurements are known to a precision of 1×10^{-4} . Unless the pressure is measured to an extremely high precision of 1×10^{-6} , the error in B''_0 is going to remain relatively large unless the measurements are made to substantially higher pressure.

The extrapolation of the pressure-volume data into a higher-pressure range is displayed in Fig. 2 in order to see the discrepancies between the equations of state, despite the questionable validity of extrapolation. Bridgman's pressure scale above 35 kbars was corrected by using the recently reported values of pressure transition points of various elements.²⁰ His values of thallium II-III at 39 kbars, barium II-III at 59 kbars, and bismuth III-V at 89 kbars, moved down to 37,²¹ 55,²² and 74-78 kbars,^{23,24} respectively. GGKE has not been shown because of its unrealistically high value of B''_0 . As shown in Fig. 2, ME₁ and ME₂ begin to deviate appreciably from other equations of state at 30 kbars. The abnormal behavior of ME₂ in the higher-pressure region is due to the dominant role of a B''_0 term in the determination of $B(P)$. KE, BE₁, and BE₂ are hardly distinguishable in the entire pressure range ($P/B_0 \approx 10$) considered.

For the improvement of equation-of-state data it would be desirable to simultaneously measure pressure-volume data by the present apparatus and $B_0(P)$ by an ultrasonic technique for the same specimen. Accurate measurements

over an extended pressure range will certainly contribute to improving data in the determination of B''_0 and B'''_0 .

CONCLUSIONS

The value of B_0 for potassium at 28.58 °C is 30.85 ± 0.05 kbars.

The value of B'_0 for potassium at 28.58 °C is 4.1 ± 0.1 . B''_0 is found to be $B''_0 \approx -0.1 \text{ kbar}^{-1}$ and hence makes a major contribution to the value of B at high pressures. It appears that the Taylor series expansion of $B(P)$ about atmospheric pressure is a slowly converging series. This is consistent with the general conclusions of Davison and Graham²⁵ that fourth-order elastic constants contribute significantly to the stress-strain response even at strains of only a few per cent.

ACKNOWLEDGMENTS

Financial support by the United States Army Research office is acknowledged. It is our pleasure to express our deep gratitude to Robert E. Terry for his able technical support.

- ¹P. W. Bridgman, Proc. Am. Acad. Arts Sci. **58**, 165 (1923).
- ²P. W. Bridgman, Proc. Am. Acad. Arts Sci. **70**, 71 (1935).
- ³P. W. Bridgman, Proc. Am. Acad. Arts Sci. **72**, 207 (1938).
- ⁴P. W. Bridgman, Proc. Am. Acad. Arts. Sci. **76**, 55 (1948).
- ⁵C. A. Swenson, Phys. Rev. **99**, 423 (1955).
- ⁶C. E. Monfort and C. A. Swenson, J. Phys. Chem. Solids **26**, 291 (1965).
- ⁷S. N. Vaidya, I. C. Getting, and G.C. Kennedy, J. Phys. Chem. Solids **32**, 2545 (1971).
- ⁸P. A. Smith and C. S. Smith, J. Phys. Chem. Solids **26**, 279 (1965).
- ⁹W. C. Overton, Jr., J. Chem. Phys. **37**, 116 (1962).
- ¹⁰J. R. Macdonald, Rev. Mod. Phys. **41**, 316 (1969).
- ¹¹J. R. Macdonald and D. R. Powell, J. Res. Natl. Bur. Stand. Sect. A **75**, 441 (1971).
- ¹²R. C. Lincoln and A. L. Ruoff, Rev. Sci. Instrum. **47**, 636 (1976).
- ¹³K. Y. Kim, L. C. Chhabildas, and A. L. Ruoff, J. Appl. Phys. **47**, 2862 (1976).
- ¹⁴L. C. Chhabildas and A. L. Ruoff, J. Appl. Phys. **47**, 4182 (1976).
- ¹⁵A. L. Ruoff, R. C. Lincoln, and Y. C. Chen, J. Phys. D **6**, 1295 (1973).
- ¹⁶L. Knopoff, in *High Pressure Physics and Chemistry*, edited by R. S. Bradley (Academic, New York, 1963), Vol. I, p. 227.
- ¹⁷O. L. Anderson, Phys. Earth Planet. Interiors **1**, 169 (1968).
- ¹⁸M. H. Rice, J. Phys. Chem. Solids **26**, 483 (1965).
- ¹⁹T. C. Fritz and R. N. Thurston, J. Geophys. Res. **75**, 1557 (1970).

- ²⁰E. C. Lloyd (Ed.), Nat. Bur. Stand. (U.S.) Spec. Publ. 326 (1971).
- ²¹G. C. Kennedy and P. N. La Mori, J. Geophys. Res. 67, 851 (1962).
- ²²J. C. Haygarth, I. C. Getting, and G. C. Kennedy, J. Appl. Phys. 38, 4557 (1967).
- ²³J. C. Haygarth, H. D. Luedemann, I. C. Getting, and G. C. Kennedy, p. 35 in Ref. 20.
- ²⁴R. N. Jeffery, J. D. Barnett, M. R. Vanfleet, and H. T. Hall, J. Appl. Phys. 38, 3172 (1966).
- ²⁵L. Davison and R. A. Graham, Phys. Rep. (Rev. Sec. Phys. Lett.) 55, 255 (1979).

Aluminum under high pressure. II. Resistivity*

J. Cheung and N. W. Ashcroft

Laboratory of Atomic and Solid State Physics, Cornell University, Ithaca, New York 14853

(Received 22 February 1979)

The scaled room-temperature resistivity [$\rho(p)/\rho(p=0)$] of crystalline aluminum is calculated as a function of pressure p . Initially the resistivity is determined as a function of volume from the standard variational treatment in which the required electron levels and distortions to the Fermi surface are described in a two-plane-wave model. To obtain the resistivity as a function of pressure, the results of this calculation are combined with a previously computed equation of state aluminum. The calculated scaled resistivity then shows a minimum at a pressure of about 25 GPa. This minimum is largely attributable to the increasing importance of distortions of the actual Fermi surface as pressure increases.

I. INTRODUCTION

The electronic structure of aluminum is relatively simple. Its bands have a largely free-electron-like character and can be interpolated quite accurately by a spatially local pseudopotential. On the other hand its Fermi surface is a complex multiply connected object that is sensitive to the choice of the pseudopotential components used to interpolate the band structure. Since the transport coefficients, and in particular the resistivity, are related to integrals over the Fermi surface, one might expect this sensitivity to become apparent if, as through the application of pressure, the pseudopotential coefficients are altered. As we shall see below, this is indeed partly the case, though in crystalline aluminum the pressure dependence of resistivity turns out to be an aggregate of some partially compensating effects. This compensation is very much a property of the metal itself (in Pb, for example, the effects we discuss should be more prominent) and also of its state (in solid aluminum the effects are far more noticeable than in the liquid state¹).

We are concerned in this paper (as in Ref. 1) with the scaled room-temperature resistivity $\rho(p)/\rho(p=0)$ of crystalline Al, at a pressure p . The natural quantity to calculate is the ratio $\rho(V)/\rho(V_0)$, where V is the volume of a sample at pressure p (and V_0 its value at $p=0$). The starting point of this calculation is the well-known variational expression² for a bound on $\rho(V)$, as described in Sec. II. For metals with complicated Fermi surfaces, the necessary computations generally require numerical procedures of matching complexity, even for relatively simple choices of the variational trial function. The result for $\rho(V)$ can certainly be expected to depend on this choice as well as on approximations made necessary for wholly numerical reasons. Much of the consequent uncertainty can, however, be reduced by focusing attention on the scaled quantity $\rho(V)/\rho(V_0)$ and, as

discussed in Sec. II, it is largely for this reason that we find it convenient to use the simplest form of trial function. Within this approximation it still remains to determine the behavior of the pseudopotential v_p , the band structure, and the Fermi surface as functions of volume. This is described in Sec. III. The piecewise two-plane-wave approximation that we use in evaluating the variational integrals is described in Sec. IV. The matrix elements appearing in the integrand also require the phonon frequencies and their volume dependences, a question that is taken up both in Secs. IV and V. The additional approximations we make in order to complete the numerical procedures are described in more detail in Sec. IV. They involve certain simplifications in the Fermi-surface geometry and in the description of the electronic levels associated with that geometry. The results are discussed in Sec. VI.

The calculations we report could be performed in principle for all simple metals. We have selected aluminum for the reasons given earlier,³ namely that its high electron density and small ion core imply an ability to sustain a high pressure without core contact. In addition, the equation of state of Al has been calculated to pressures in excess of 300 GPa (3 Mbar). This information allows us to convert from $\rho(V)/\rho(V_0)$ to $\rho(p)/\rho(p=0)$ and hence arrive at the curves described in Sec. V.

II. RESISTIVITY OF SIMPLE METALS

For a metal of valence Z , the standard variational reduction of the Boltzmann equation yields for the resistivity at high temperatures the expression²

$$\rho \leq \frac{a_0^2 \pi}{e^2} \frac{2\pi Z}{a_0 k_F} \frac{\frac{2\pi}{k_F}}{\left[\int d^3x / v_p(\vec{v}/v_p) \Phi(x) \right]^2} 2\beta \delta_F \frac{m}{M} I, \quad (1)$$

where

$$I = \int \frac{d^2x_1}{v_1/v_F} \int \frac{d^2x_2}{v_2/v_F} [\Phi(\vec{x}_2) - \Phi(\vec{x}_1)]^2 \\ \times \sum_{\lambda} \frac{|\epsilon_{\lambda}(\vec{x}_2 - \vec{x}_1) \cdot (\vec{x}_2 \mid \nabla w \mid \vec{x}_1)|^2}{\sinh^2[\frac{1}{2}\beta i\omega_{\lambda}(\vec{x}_2 - \vec{x}_1)]}.$$

Here Φ is the trial function used in obtaining the bound for ρ , k_F is the magnitude of the Fermi wave vector, v_F is the Fermi velocity, \mathcal{E}_F is the Fermi energy, $\beta = 1/k_B T$, M is the mass of an ion, and ω_{λ} and ϵ_{λ} refer to the frequency and polarization of phonons with reduced wave vector \vec{x} . We use scaled wave vectors $\vec{x} = \vec{k}/2k_F$ and a scaled pseudopotential $w = v_F/(\frac{2}{3}\mathcal{E}_F)$, where $-\frac{2}{3}\mathcal{E}_F$ is the known long-wavelength limit of the pseudopotential form factor. The quantity $a_0\hbar/e^2$ is the atomic unit of resistivity and has the value $21.7 \mu\Omega\text{cm}$.

In the one-plane-wave approximation the quantity I in (1) can be written

$$2\beta \mathcal{S}_F \frac{m}{M} I = \int \frac{d^2x_1}{v_1/v_F} \int \frac{d^2x_2}{v_2/v_F} [\Phi(\vec{x}_2) - \Phi(\vec{x}_1)]^2 \\ \times |w(\vec{x}_2 - \vec{x}_1)|^2 S(\vec{x}_1, \vec{x}_2), \quad (2)$$

where $S(\vec{x}_1, \vec{x}_2)$ is the one-phonon structure which takes the form

$$S(\vec{x}) = S(\vec{x}_2 - \vec{x}_1) = 2\beta \mathcal{S}_F \frac{m}{M} \sum_{\lambda} [\epsilon_{\lambda}(\vec{x}) \cdot \vec{x}]^2 \\ \times \sinh^2[\frac{1}{2}\beta i\omega_{\lambda}(\vec{x})]. \quad (3)$$

The sum in (3) is over the possible polarizations λ , and the integral is over the actual Fermi surface which in the case of the alkali metals, for example, can be very well approximated by a sphere. For the polyvalent metals, however, the shape of the Fermi surface must be taken into account since a substantial fraction of the free-electron Fermi surface can actually be lost.

It has been shown^{4,5} that for the calculation of high-temperature resistivity the effects of anisotropy in the choice of trial functions are of diminishing importance. As a consequence of this observation we have used a trial function of the form

$$\Phi(\vec{x}) \propto \vec{v}(\vec{x}) \cdot \hat{z}, \quad (4)$$

(where \hat{z} is parallel to the electric field) recognizing that although the calculated resistivity must necessarily be in excess of the actual value, the effect of the approximation on $\rho(p)/\rho(0)$, as noted earlier, will be much reduced. Although this choice for Φ greatly simplifies the numerical work, a generalization to more complex forms for Φ is quite straightforward.

Given (4) as the trial function then for a cubic system, (1) becomes

$$\rho \approx \frac{a_0\hbar}{e^2} \frac{2\pi Z}{a_0 k_F} \left(\frac{m_{\text{eff}}}{m} \right)^2 2\beta \mathcal{S}_F \frac{m}{M} I, \quad (5)$$

where

$$\frac{m}{m_{\text{opt}}} = \frac{\int d\vec{s}_{\vec{k}} v(\vec{k})}{s_0 v_F} \quad (6)$$

defines the optical effective mass which can be calculated directly.⁶ In (6) s_0 is the area of the free-electron Fermi surface ($s_0 = 4\pi k_F^2$). Attention then reverts to the remaining double surface integral in I , which we shall treat in a two-plane-wave approximation. Were the Fermi surface spherical, a one-plane-wave treatment would suffice and the identity

$$\int_{s_F} d\vec{s}_{\vec{k}} \int_{s_F} d\vec{s}_{\vec{k}'} \\ = \int d\vec{k} \int d\vec{k}' \delta(k - k_F) \delta(k' - k_F) \quad (7)$$

reduces the problem to a single volume integral over $\vec{q} = \vec{k} - \vec{k}'$. With these simplifying features the calculation of the resistivity in the alkali metals is itself relatively simple. In the polyvalent metals, however, transformation (7) will not correctly treat transitions involving parts of the Fermi surface that depart from a simple spherical character. On the other hand (as we shall see) there are portions of the actual Fermi surface that remain very spherical and contributions from these can be transformed into a corresponding volume integral. The remaining (nonspherical) portions must, however, be treated by evaluating (1) directly.

III. PSEUDOPOTENTIAL AND FERMI-SURFACE GEOMETRY

In the two-plane-wave approximation to be discussed in Sec. IV, the electronic energy \mathcal{E} for level k is given near zone planes by the solutions of

$$\begin{vmatrix} \mathcal{E}_{\vec{k}} - \mathcal{E} & V_s(\vec{k}) \\ V_s(\vec{k}) & \mathcal{E}_{\vec{k}-\vec{k}} - \mathcal{E} \end{vmatrix} = 0, \quad (8)$$

where \vec{k} is the reciprocal-lattice vector under consideration and $\mathcal{E}_{\vec{k}} = (\hbar^2/2m)k^2$. $V_s(\vec{k})$ is related to the screened pseudopotential $v_s(\vec{k})$ by $V_s(\vec{k}) = \Omega_0^{-1} v_s(\vec{k})$, where Ω_0 is the volume of the primitive cell: by choice $V_s(0) = 0$.

In order to calculate the resistivity we need to know the form of the pseudopotential $v_s(k)$ throughout the range $0 \leq k \leq 2k_F$. For aluminum, a one-parameter empty-core potential serves adequately.⁷ In \vec{k} space it can be written (with $x = k/2k_F$ and $s = 2k_F r_c$)

$$v_s(\vec{x}) = \frac{-\pi Ze^2}{x^2 k_F^2 \epsilon(x)} \cos(sx). \quad (9)$$

Here r_c is the parameter usually referred to as

the "empty-core radius." The value of r_c should be close to the size of the ion core on physical grounds and is around $1.12a_0$ for aluminum. For the dielectric function $\epsilon(x)$, we take⁸

$$\epsilon(x) = 1 + H(x)[1 - G(x)],$$

with

$$H(x) = (\pi a_0 k_F x^2)^{-1} \left(\frac{1}{2} + \frac{1-x^2}{4x} \ln \left| \frac{1+x}{1-x} \right| \right) \quad (10)$$

and

$$G(x) = x^2/(2x^2 + \xi).$$

The exchange-correlation parameter ξ is given by⁸

$$\xi = 1/(1 + \alpha r_s),$$

where r_s is the electron spacing radius defined by $\Omega = \frac{4}{3}\pi Z r_s^3$, and $\alpha \approx 0.025$.

The screened pseudopotential form factor for aluminum is plotted in Fig. 1. In the same figure we also show the corresponding quantity for the compressed metal with $V/V_0 = 0.7$. On plotting w as a function of x we see that the node (where $w = 0$) moves to lower reduced wave vector as the metal is compressed. Correspondingly the Fourier coefficients $V_s(111)$ and $V_s(200)$ are seen to increase. While pseudopotential theory suggests that r_c should be energy dependent,⁹ the energy

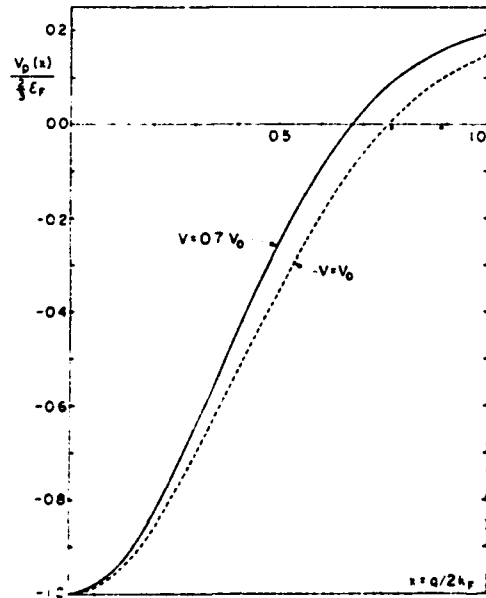


FIG. 1. Pseudopotential form factor of aluminum for $V/V_0 = 1.0$ and $V/V_0 = 0.7$. Screening by conduction electrons [Eq. (10)] the appropriate densities is taken into account, the empty-core radius r_c is $1.12a_0$. The arrows mark the location of the reciprocal-lattice vectors $K = (1, 1, 1)$ and $(2, 0, 0)$.

dependence is expected to be small since r_c reflects the size of the ion core which should not change greatly with pressure-induced changes in its environment. Holding r_c fixed is tantamount to ignoring such small additional energy dependence.

With the "new" values of $V_s(111)$ and $V_s(200)$ (for the compressed metal) we can use (8) again to map out the Fermi surface. Because of the different values of the new Fourier coefficients, the geometry of the Fermi surface of the compressed metal can be different from that of the metal under normal conditions. We take this into consideration.

IV. TWO-PLANE-WAVE APPROXIMATION

The evaluation of the double surface integral in (1) has been a major numerical obstacle in most of the calculations of the resistivity of polyvalent metals. Because of the complex geometry of the Fermi surface of these metals a large number of surface-area elements is necessary to characterize the surface accurately.¹⁰⁻¹² For the high-temperature transport coefficients the problem of the Fermi-surface anisotropy is less,^{4,5} and in view of this we have chosen to carry out the calculations by means of a two-plane-wave approximation which has also been used by other authors in similar model calculations.^{13,14} Although at some points on the Fermi surface three or even four orthogonalized plane waves are needed to give an adequate description of the finer distortions,¹⁵ the amount of surface requiring this more detailed description is small compared with the total Fermi-surface area. Essentially, our approximation treats each of the many Bragg planes in turn and calculates the contribution to the resistivity with the electronic levels described by the linear combination of plane waves

$$\Psi_{\vec{k}}(\vec{r}) = \sin \theta_{\vec{k}} e^{i \vec{k} \cdot \vec{r}} + \cos \theta_{\vec{k}} e^{i (\vec{k} - \vec{K}_0) \cdot \vec{r}}. \quad (11)$$

The total resistivity is then the sum of the umklapp contributions of the individual reciprocal-lattice vector (\vec{K}) and the normal contribution. Our numerical calculations show that the normal contribution is only a small part of the total resistivity and for this it is quite adequate to use the simple one-plane-wave treatment.

Consider the umklapp processes made possible by transitions involving a particular reciprocal-lattice vector \vec{K} . The umklapp processes are those for which the initial levels \vec{k}_1 originate on the Fermi surface and the final levels \vec{k}_2 end on the remapped surfaces, i.e.,

$$\vec{k}_2 - \vec{k}_1 = \vec{q} - \vec{K} \quad (12)$$

with \vec{q} in the first Brillouin zone. Some umklapp

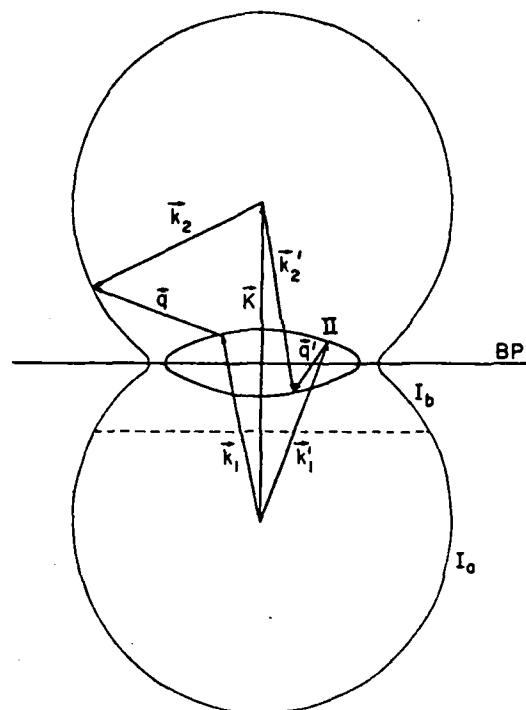


FIG. 2. Two possible umklapp processes are shown here in the single-Bragg-plane (BP) approximation ($\vec{k}_1 \rightarrow \vec{k}_2$; $\vec{k}_1 - \vec{k}_2$). Note that the Fermi surface is divided up into three parts for computational purposes as described in the text.

processes are pictured in Fig. 2 where we also see that the Fermi surface is split into two sections because of the finite value of v_K .

The parameter θ describing the electron levels in (11) is given by

$$\tan \theta_K = \eta \pm \text{sgn}(v_K)(\eta^2 + 1)^{1/2},$$

with

$$\eta = [4S_F / |V_p(\vec{K})|] \\ \times [\vec{x} \cdot (\vec{K}/2k_F) - \frac{1}{2}(K/2k_F)^2], \quad x = k/2k_F. \quad (13)$$

The (\pm) in (13) signify the band index, with $(+)$ for the second band and $(-)$ for the first.

The matrix element M required in (1) is in general given by

$$-i\epsilon_\lambda(\vec{x}_2 - \vec{x}_1) \cdot (\vec{x}_2 \mid \vec{\nabla} \psi \mid \vec{x}_1)$$

when the wave functions are normalized. Before we consider this further we will first describe the approximations we make concerning the phonon frequencies and polarizations. With the exception of those along the major symmetry axes, the phonons have polarizations that are neither pure longitudinal nor pure transverse. However, the large number of symmetry axes present in the

Brillouin zone of the cubic structures guarantees that throughout the zone the phonons have polarizations that are usually quite close to being purely longitudinal or purely transverse. It thus seems reasonable to replace the phonon dispersion curves with one longitudinal branch and two identical transverse branches with dependence on the magnitude of \vec{q} alone, these branches being appropriately weighted averages of the frequencies along the major symmetry axes. Implicit in this is the subsequent replacement of the zone by the Debye sphere. The individual phonon frequencies are calculated from an eight-shell axially symmetric model with *experimental force-constants* obtained from experiments at 300 °K.¹⁶ This procedure inevitably introduces errors into the final result, but the uncertainties are not expected to be large, especially if the main interest centers on the way resistivity changes as a consequence of the variation of the frequencies themselves.

With this approximation, the scaled longitudinal and transverse matrix elements (squared) are then given by

$$(2k_F)^2 (\frac{2}{3} S_F)^2 M_L^2(\vec{K}_2, \vec{K}_1) \\ = \{q V_p(\vec{q})(S_1 S_2 + C_1 C_2) + q V_p(\vec{q} - \vec{K}) S_2 C_1 \\ + q V_p(\vec{q} + \vec{K}) S_1 C_2 + \vec{q} \cdot \vec{K} [V_p(\vec{q} + \vec{K}) S_1 C_2 \\ - V_p(\vec{q} - \vec{K}) S_2 C_1]^2\}^2 \quad (14)$$

and

$$(2k_F)^2 (\frac{2}{3} S_F)^2 \sum_i M_T^2(\vec{K}_2, \vec{K}_1) \\ = K^2 [1 - (\vec{q} \cdot \vec{K})^2] [V_p(\vec{q} + \vec{K}) S_1 C_2 \\ - V_p(\vec{q} - \vec{K}) S_2 C_1]^2,$$

where $S_i = \sin \theta_i$ and $C_i = \cos \theta_i$, with $i = 1, 2$. Given the trial function (4) the quantity $[\Phi(\vec{k}_2) - \Phi(\vec{k}_1)]^2$ appearing in (1) is determined by

$$(2k_F)^2 [\Phi(\vec{K}_2) - \Phi(\vec{K}_1)]^2 \\ = q^2 + 2\vec{q} \cdot \vec{K} (C_1^2 - C_2^2) + K^2 (C_2^2 - C_1^2)^2. \quad (15)$$

If the band gaps are small (as in aluminum) then only a small region of the Fermi sphere needs to be described in the two-plane-wave formalism, the rest being essentially free-electron-like. Considerable computational effort can be saved if we divide up the first band into two parts (see Fig. 2), I_a and I_b , in which I_a is the part of the first band where a one-plane-wave description would be adequate while I_b is the part that requires the two-plane-wave description (as determined by a suitably chosen criterion¹⁷). The processes involving initial states on I_a and final states on the remapped part of I_b are essentially free-electron-like and

will be dealt with separately. Contributions from processes involving H and I_b will then be computed by directly evaluating the double integral.

The double Fermi-surface integrals required for the evaluation of (1) thus have contributions from the normal processes (which are small in the case of aluminum), umklapp processes in the two-plane-wave single-Bragg-plane approximation, and umklapp processes that can be considered as involving free-electron-like levels.

V. APPLICATION TO COMPRESSED ALUMINUM

As mentioned above, the phonon frequencies at normal conditions (300 K and zero pressure) are generated by an axially symmetric force-constant model. The effects of the volume change on the phonon frequencies themselves) can be calculated in a straightforward manner from the dynamical matrices.^{18,19} In the polyvalent metals it is well known that such a calculation is computationally time consuming as a large number of terms is needed for the dynamical matrices to converge. We choose instead to scale all the frequencies with the bulk experimental Grüneisen parameter γ (2.35 for aluminum²⁰), i.e.,

$$\omega(q, V) = \omega_0(q) \left(1 + \gamma \frac{V_0 - V}{V} \right). \quad (16)$$

In (16) $\omega(q, V)$ is the phonon frequency of the wave vector q at the compressed volume V and ω_0 is the observed frequency at the zero-pressure volume V_0 . Though a crude approximation for the changes in the frequencies themselves, it should be satisfactory for the quotient $\rho(V)/\rho(V_0)$ involving ratios of integrals accompanying such changes. A more realistic approach is to take into account the changes in the elastic constants in the evaluation of the changes in the phonon frequencies.²¹

The numerical evaluation of Eq. (1) also involves the computation of the factor $(m_{opt}/m)^2$. From Eq. (6) we see that this factor is a measure of the distortions in the Fermi surface. On the other hand, we note that in evaluating the umklapp contributions to the double surface integral, the Fermi surface used is *not* the actual fully distorted Fermi surface. For each particular Bragg plane (at, say, $\frac{1}{2}\vec{K}$) only the distortions associated with a given $V_p(\vec{K})$ are taken into account. This amounts to using a Fermi surface with an area *larger* than the actual one (in our two-plane-wave model, the actual Fermi surface would have distortions resulting from 14 Bragg planes). We can estimate the combined effects of the necessary further reduction in Fermi-surface area as follows.²² We note that, with the trial function given by (4), the double surface integral in (1) takes the form

$$\int \frac{ds_1}{v_1} \int \frac{ds_2}{v_2} |\vec{v}_2 - \vec{v}_1|^2 \dots, \quad (17)$$

where the rest of the integrand has a somewhat weaker dependence on the location on the Fermi surface. The ratio of

$$\int \frac{ds_1}{v_1} \int \frac{ds_2}{v_2} |\vec{v}_2 - \vec{v}_1|^2$$

to a corresponding quantity for the free-electron case is thus an approximation of the correction factor required. Using inversion symmetry, we have

$$\begin{aligned} & \frac{\int (ds_1/v_1) \int (ds_2/v_2) |\vec{v}_2 - \vec{v}_1|^2}{\int (ds_1^0/v_1^0) \int (ds_2^0/v_2^0) |\vec{v}_2^0 - \vec{v}_1^0|^2} \\ &= \frac{\int (ds/v) \int ds v^2}{\int (ds^0/v^0) \int ds^0 v^0}, \end{aligned} \quad (18)$$

where $\int ds v^2 / \int ds^0 v^0$ is just m/m_{opt} while $(\int ds/v) / (\int ds^0/v^0)$ is commonly referred to as the specific-heat effective mass m_{sh}/m . Combining this with the factor $(m_{opt}/m)^2$, we arrive at a total correction factor $f = (m_{opt}/m)(m_{sh}/m)$. In the two-plane-wave model m_{opt} and m_{sh} can be obtained without further approximation in closed form⁶:

$$\begin{aligned} \frac{m}{m_{opt}} &= 1 - \sum_K \frac{1}{2} \frac{K}{2k_F} \frac{|V_p(K)|}{S_F} \left\{ \left[\frac{\pi}{2} - \sin^{-1} \left(\frac{2V_p(K)}{\omega_0} \right) \right] \right. \\ &\quad \left. + \frac{|V_p(K)|}{2S_K} \left[\frac{\omega_0}{2\omega_1} + \frac{3\omega_1}{2\omega_0} - 2 - \ln \left(\frac{\omega_1}{\omega_0} \right) \right] \right\}, \end{aligned}$$

where

$$\omega_0 = 2[S_K S_F + V_p^2(K)]^{1/2} - S_K \quad (19)$$

and

$$\omega_1 = 2[S_K S_F + V_p^2(K)]^{1/2} + S_K.$$

Further,

$$\frac{m_{sh}}{m} = 1 - \frac{1}{2} \sum_K (1 - X - \{1 + X^2 - [4X^2 + \frac{3}{4}\omega^2(X)]^{1/2}\}^{1/2}),$$

where $X = K/2k_F$. These formulas then serve as an indication of the accuracy of our numerical procedure within the two-plane-wave model. The results are listed in Table I. We note also that the scaled correction factors, i.e., $r(r_s) f(r_{s0})$, compare very well. The resistivity of aluminum as a function of compressed volume is plotted in Fig. 3. Here we display the results using both the correction factors from the closed form solutions (f_s) and those from the numerical calculations (f_n).

The equation of state of aluminum has been obtained by Friedli and Ashcroft.³ They examined most of the common crystal structures and concluded that for the pressure range they considered (up to and above 300 GPa) the fcc structure is that of lowest calculated energy. We can numerically

TABLE I. Quantities m_{opt}/m and m_{sh}/m evaluated in the two-plane-wave model. Both closed-form (analytical) and numerical results are listed. The quantity f is defined by $f = (m_{\text{opt}}/m)(m_{\text{sh}}/m)$. (Note: $r_s = 2.073$.)

$r_s(a_n)$	V/V_0	m_{opt}/m		m_{sh}/m		$f(r_s)/f(r_{s0})$	
		Analytical	Numerical	Analytical	Numerical	Analytical	Numerical
2.073	1.00	1.370	1.305	0.985	0.987	1.00	1.00
2.001	0.90	1.644	1.561	0.976	0.979	1.19	1.18
1.924	0.80	2.070	1.910	0.964	0.966	1.48	1.43
1.841	0.70	2.819	2.552	0.947	0.949	1.98	1.88

eliminate r_s between this equation of state and the resistivity variation we obtain in this calculation to arrive at a scaled resistivity curve which is shown in Fig. 4. Unfortunately, we have not been able to locate experimental data on the pressure variation of the resistivity of crystalline aluminum. The data of Bridgman summarize the measurement of relative resistance rather than the relative resistivity.^{23,24} However, we can get an estimate of the experimental value of

$$[\Delta(\rho/\rho_0)/\Delta(V/V_0)]_{V/V_0=1}$$

from the Bridgman data by using the approximate equation for an isotropic cubic crystal (roughly applicable to the experimental arrangement of

Bridgman):

$$\left. \frac{\Delta(\rho/\rho_0)}{\Delta(V/V_0)} \right|_{V/V_0=1} = \left. \frac{\Delta(R/R_0)}{\Delta(V/V_0)} \right|_{V/V_0=1} + \frac{1}{3}. \quad (20)$$

With this equation we get 2.3 for the experimental value²⁵ of $\Delta(\rho/\rho_0)/\Delta(V/V_0)$ and this should be compared with the theoretical result of 2.5 obtained here.

VI. DISCUSSION AND CONCLUSION

Our calculations, though they describe quite well the qualitative trend of the behavior of resistivity under pressure (as compared with experiments at low pressures), do not yield particularly accurate numerical results for the resistivity itself. At normal conditions the resistivity $\rho(0)$ is overestimated by 50% (the computed values are 4.2 and 4.0

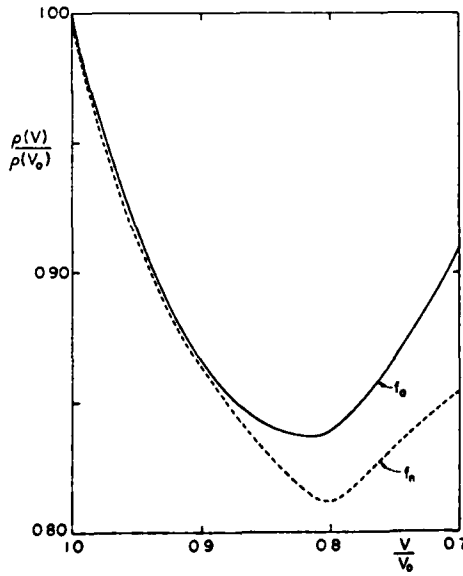


FIG. 3. Scaled resistivity of aluminum as a function of compressed volume at $T = 300^\circ\text{K}$ in the single-Bragg-plane two-plane-wave approximation. The curve labeled f_0 is obtained by applying the Fermi-surface-area correction factor in closed form; the f_n curve is obtained with the correction factor obtained numerically (see text).

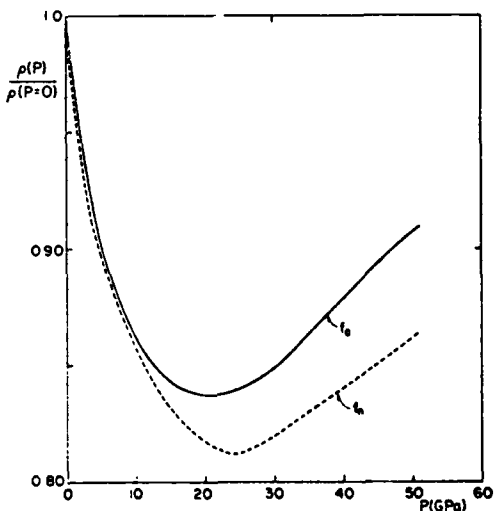


FIG. 4. Scaled resistivity of aluminum as a function of pressure. The curves are obtained by numerically eliminating the volume between the curves shown in Fig. 3 with the equation of state of aluminum. The equation of state is obtained by the procedure described in Ref. 3.

$\mu\Omega\text{cm}$ with the correction factors f_s and f_n , respectively) and is characteristic of the errors encountered in the equivalent calculation in the liquid state.¹ The discrepancy can be attributed to the approximations we have made and to the choice of trial function. The Fermi surface over which we perform our double surface integral is at best a rough approximation of the real Fermi surface which has a much more complex geometry. Our approximation of a single Bragg plane allows for more transitions to be included as the Fermi surface thus generated has a larger area than the real Fermi surface. This additional surface is only approximately accounted for in our treatment of applying the correction factor (18). Another source of error can be traced to the replacement of the phonon frequencies by three branches (one longitudinal and two identical transverse) and the replacement of the first Brillouin zone by a Debye sphere. This simplifies the problem but at the same time discounts all the effects of phonon anisotropy. The errors introduced by using a single Grüneisen parameter to describe the phonon frequency changes will be averaged out to a certain extent (at least for small volume changes) as an integral is performed to arrive at the resistivity. Furthermore, we note that the two-plane-wave approximation is not adequate for some electronic levels, especially those near the zone edges and corners. The electronic levels near the symmetry point W , for instance, require four plane waves for an adequate characterization. A realistic description of the electronic levels is attempted only near the Bragg plane under consideration—and this is only done crudely—a simplification¹ at inevitably introduces errors into our results. We note, however, that the fraction of the Fermi surface that is close to a Bragg plane is already small. Thus, we can expect that the fraction that lies near the intersection of two or three of these Bragg planes to be smaller still. Further Bragg planes [the next class is (220)] are excluded from our consideration as they lie outside the Fermi sphere. The inadequacy of the trial function we use necessarily leads to overestimation of the resistivity.

However, we believe our results for the scaled quantity have quantitative validity in the description they give of the *changes* in the resistivity as pressure is applied, the previous objections notwithstanding. The reason is that when we consider the changes brought about by the application of pressure then the relative uncertainties in each of the considerations should be considerably reduced.

The results of our calculation are somewhat interesting in that the resistivity of aluminum shows

a minimum as the metal is compressed. The mechanisms that cause this minimum are not the same as those believed to account for the resistivity minima in the alkali metals. In the latter case the admixture of d states in the levels at the Fermi energy is believed to be responsible,^{23,26-29} while in the case of aluminum the minimum appears to be a manifestation of changes in the Fermi-surface geometry. In our simple model of the electron-ion pseudopotential under compression we see that for all the compressed volumes considered the reduced Fourier coefficients $r_p(111)/\frac{2}{3}\epsilon_F$ and $r_p(200)/\frac{2}{3}\epsilon_F$ increase as the metal is compressed. These increases cause the reduction in Fermi-surface area (as compared to the free-electron sphere) to increase from about 14% to about 38% when the volume of the sample is reduced by 30%. The values of the reduced Fourier coefficients and the Fermi surface area reductions are listed in Table II.

It is quite clear that a more careful treatment of the resistivity variation requires that the Fermi-surface distortions be fully taken into account. If the Fermi-surface effects are included (as described in Sec. V), we see that the simple picture of a one-plane-wave treatment needs to be modified. In addition to the (main) effect of reductions in resistivity stemming from increases in phonon frequencies²¹ we have an offsetting effect from the increase in the distortions of the Fermi surface which ultimately reverses the trend. The net correction factor that should be applied for these distortions should be

$$f = (m_{\text{opt}}/m)(m_{\text{sh}}/m)$$

instead of the $(m_{\text{opt}}/m)^2$ appearing in Eq. (1) because of a corresponding reduction in the region of integration for the double surface integral in Eq. (1). As m_{sh}/m remains near unity for all the values of r_s considered, we see that the correction factor is reflected by the increase (as a function of compression) of the optical mass. The two effects together cause a resistivity minimum at $V/V_0 \approx 0.8$ which would be absent in the one-plane-wave treatment.

TABLE II. Reduced Fourier coefficient $r_p(111)/\frac{2}{3}\epsilon_F$ and $r_p(200)/\frac{2}{3}\epsilon_F$ and the reduction in Fermi-surface area as a function of compressed volume. The two-plane-wave model is used to compute the Fermi-surface (FS) area reductions.

$r_s(a_n)$	V/V_0	$r_p(111)/\frac{2}{3}\epsilon_F$	$r_p(200)/\frac{2}{3}\epsilon_F$	FS Reduction
2.073	1.00	0.0050	0.0949	14%
2.001	0.90	0.0322	0.1144	22%
1.924	0.80	0.0555	0.1350	29%
1.84	0.70	0.0870	0.1564	38%

While the validity of the simple one-plane-wave treatment can be justified for high temperatures and zero pressure, we have found that in dealing with the compressed metal a more realistic treatment taking into consideration the Fermi-surface distortions is plainly required. As discussed above, this differs from the situation in the alkali metals where the distortions in the Fermi surface are second-order effects. As another example of a polyvalent metal we may consider Pb whose Fourier coefficients (or rather their magnitudes) are expected to decrease as the metal is compressed.³⁰ Therefore, both the Fermi-surface distortion (as reflected in the optical mass) and the increase in phonon frequencies cause the re-

sistivity to decrease as a function of pressure and we would expect the pressure coefficient of Pb to be larger than the result from a one-plane-wave calculation. Thus, for the polyvalent metals our single-Bragg-plane and two-plane-wave approximation is a first step in taking these distortions into account and already shows that among the simple metals some qualitatively different effects can be expected.

ACKNOWLEDGMENT

This research has been supported by the United States Army Research Office, Research Triangle Park, North Carolina, under Grant No. DAAG29-78-G-0040.

- *See AIP document no. PAPS PRBMDO-20-2991-51 for a lengthier version of this paper which includes a more detailed explanation of the calculational procedures. Order by PAPS number and journal reference from the American Institute of Physics, Physics Auxiliary Publication Service, 335 East 45th Street, New York, New York 10017. The price is \$1.50 for each microfiche (98 pages), or \$5 for photocopies of up to 30 pages with \$0.15 for each additional page over 30 pages. Air mail additional. Make checks payable to the American Institute of Physics.
- ¹J. Cheung and N. W. Ashcroft, Phys. Rev. B 18, 559 (1979).
²J. M. Ziman, *Electrons and Phonons* (Oxford University, London, 1960).
³C. Friedli and N. W. Ashcroft, Phys. Rev. B 12, 5552 (1975).
⁴J. Black and D. L. Mills, Phys. Rev. B 9, 1459 (1974).
⁵J. W. Ekin and A. Bringer, Phys. Rev. B 7, 4468 (1973).
⁶N. W. Ashcroft and K. Sturm, Phys. Rev. B 3, 1398 (1971).
⁷N. W. Ashcroft, Phys. Lett. 23, 48 (1966).
⁸D. J. W. Geldart and S. H. Vosko, Can. J. Phys. 44, 2137 (1966); 45, 2229(E) (1966); D. C. Wallace, Phys. Rev. 192, 778 (1969).
⁹V. Heine, Solid State Phys. 24, 1 (1970).
¹⁰Y. Bergman, M. Kaveh, and N. Wiser, Phys. Rev. Lett. 32, 606 (1974).
¹¹A. B. Meador and W. E. Lawrence, Phys. Rev. B 15, 1550 (1977).
¹²H. K. Leung, F. W. Kus, N. McKay, and J. P. Carbotte, Phys. Rev. B 16, 4358 (1977); H. K. Leung, J. P. Carbotte, D. W. Taylor, and C. R. Leavens, Can. J. Phys. 54, 1585 (1976).
¹³W. E. Lawrence and J. W. Wilkins, Phys. Rev. B 6, 4466 (1972).
¹⁴H. B. Huntington and W. C. Chan, Phys. Rev. B 12,

- 5423 (1975); W. C. Chan and H. B. Huntington, *ibid.* 12, 5441 (1975).
¹⁵N. W. Ashcroft, Philos. Mag. 8, 2055 (1963).
¹⁶G. Gilat and R. M. Nicklow, Phys. Rev. 143, 487 (1966).
¹⁷The criterion used is that the electron velocity (calculated in the approximation used) on I_e differs from v_F , the Fermi velocity, by less than 1%.
¹⁸D. C. Wallace, Phys. Rev. 187, 991 (1969).
¹⁹P. V. S. Rao, J. Phys. Chem. Solids 35, 669 (1974).
²⁰V. P. Singh and M. P. Hemkar, J. Phys. F 7, 761 (1977). References for experimental results of the bulk Grüneisen parameter are cited in this work.
²¹Such a calculation was done for the alkali metals by M. Kaveh and N. Wiser [Phys. Rev. B 6, 3648 (1972)].
²²These effects are also discussed in Refs. 13 and 14. The way we allow for the Fermi-surface distortions is different from that of Ref. 14. See also, N. W. Ashcroft, Phys. Rev. B 19, 4906 (1979).
²³F. P. Bundy and H. M. Strong, Solid State Phys. 13, 81 (1962).
²⁴P. W. Bridgman, *The Physics of High Pressure* (Bell, London, 1949).
²⁵Data taken from Ref. 23.
²⁶H. G. Drickamer, Solid State Phys. 17, 1 (1965).
²⁷J. S. Dugdale, in *Advances in High Pressure Research*, edited by R. S. Bradley (Academic, London, 1969), Vol. 2, 101.
²⁸N. H. March, in *Advances in High Pressure Research*, edited by R. S. Bradley (Academic, London, 1969), Vol. 3, p. 241.
²⁹J. M. Dickey, A. Meyer, and W. H. Young, Proc. Phys. Soc. Lond. 92, 460 (1967).
³⁰The pseudopotential for Pb is discussed, e.g., by M. L. Cohen and V. Heine [Solid State Phys. 24, 38 (1970)].

Core polarization and the equation of state of potassium

J. Cheung* and N. W. Ashcroft

Laboratory of Atomic and Solid State Physics, Cornell University, Ithaca, New York 14853

(Received 13 April 1981)

We calculate the zero-temperature equation of state of potassium with a model Hamiltonian that includes core-polarization effects. Density fluctuations in the ion cores lead to van der Waals interactions that are dynamically screened by the valence electrons. They also lead to screening of other static interactions, effects that are incorporated through the use of a background dielectric function $\epsilon_c(q)$. Inclusion of core-polarization effects yields significant improvement between the theoretical and experimental equations of state, particularly at high pressures.

I. INTRODUCTION

In calculations of the thermodynamic functions of the simple metals it is common to assume that core-polarization effects can be neglected, an assumption that is normally justified on the grounds that the electrons in the corresponding ions are tightly bound and in consequence not significantly polarizable. It then follows that the dispersion forces and the effects of any background dielectric shielding associated with the internal structure of the ions should be small, at least in comparison with the much stronger Coulomb interactions and electron-gas properties. Under normal conditions these assumptions are usually valid: The screened van der Waals interactions, for example, produce only a slight softening of the repulsive part of the pseudopotential-derived ion-ion potential.¹ At high pressures, however, where interionic separations are much reduced, the softening of such potentials can have noticeable effects, as we shall see here. In addition, the likely importance of the background screening can be gauged by examining the quantity $\epsilon_c(0) \approx 1 + 4\pi n_i \alpha$, where α is an ionic polarizability and n_i is the ionic number density. In the alkali metal series this does not depart appreciably from unity (the range is about 1.01–1.27); nevertheless, such departures can lead to quite significant corrections to the various terms comprising the total energy of a metal,² particularly at high pressure where n_i has been increased.

In a previous paper³ (referred to as I) we derived a model Hamiltonian to treat the problem of a system of interacting dipoles and electrons for use in the calculation of thermodynamic and structural properties of simple metals. It was shown there

that the collective core-core excitations give rise to screened polarization waves, and the lowest-order dispersion forces associated with these waves are the screened van der Waals interactions. It was also shown that in addition to participating in physical processes involving collective excitation and dynamic screening, the polarizable ions screen all the static interactions. At the microscopic level the system of ions constitutes an inhomogeneous dielectric which for long-ranged interactions in situations of high symmetry may be reasonably well approximated by a dielectric continuum with dielectric function $\epsilon_c(q)$. In this paper we shall apply the principal results of I to be the case of potassium which has a rather substantial ionic polarizability (see Table II of Ref. 1). It also has a high compressibility which makes it well suited to the present calculation.

The paper is organized as follows: In Sec. II, the key results for the total energy of a simple metal with polarizable ions are restated. In Sec. III we introduce the additional approximation needed to evaluate the zero-temperature isotherm. This requires us to address the form of the static background dielectric function $\epsilon_c(q)$ for a dielectric continuum representing the ions, as well as the atomic polarizabilities themselves. The results are discussed in Sec. IV.

At high compression the effects we are discussing are quite significant, as will be seen. It should be noted here that by ignoring core-polarization effects entirely it is still quite possible to obtain a detailed quantitative description of the elastic properties of the alkali metals^{4,5} using pseudopotential methods. We shall see below that the explanation for this minor paradox is simply the observation that for modest compressions the correction terms arising

from core polarization effects can be almost entirely absorbed into the standard zero pressure fitting procedure in which the aggregate of all long-wavelength terms is adjusted to an experimental datum. The volume dependence of the core-polarization terms is, however, sufficiently different that under more extreme circumstances, such as the treatment of shock Hugoniots and the determination of Grüneisen parameters, this procedure may require reexamination.

II. GROUND-STATE ENERGY OF A SIMPLE METAL

We shall neglect the energy associated with the nuclear degrees of freedom⁵: The Hamiltonian for a simple metal of valence Z and of volume Ω whose ions are polarizable can then be written^{1,3}

$$H = \sum_i \frac{p_i^2}{2m} + \frac{1}{i} \sum_{\vec{q} \neq 0} \frac{v_c(q)}{\Omega \epsilon_c(q)} \hat{\rho}^*(\vec{q}) \hat{\rho}^0(-\vec{q}) \quad (1a)$$

$$+ \sum_{\vec{q} \neq 0} \frac{v_{pe}(q)}{\Omega \epsilon_c(q)} \hat{\rho}^0(\vec{q}) \hat{\rho}^0(-\vec{q}) \quad (1b)$$

$$+ \frac{1}{i} \sum_{\vec{q} \neq 0} \frac{Z^2 v_c(q)}{\Omega \epsilon_c(q)} [\hat{\rho}^0(\vec{q}) \hat{\rho}^0(-\vec{q}) - N] \quad (1c)$$

$$+ NZE_0 + \frac{1}{i} \sum_{\vec{R}, \vec{R}'} \phi_L^*(\vec{R} - \vec{R}') \quad (1d)$$

As described in I the terms here have the following meaning: Term (1a) is the Hamiltonian of an interacting electron gas in a neutralizing dielectric continuum with dielectric constant $\epsilon_c(q)$. The valence-electron density operator is $\hat{\rho}^0(\vec{q}) = \sum_i e^{i\vec{q} \cdot \vec{r}_i}$; the Coulomb interaction is $v_c(q) = 4\pi e^2/q^2$. Term (1b) is a characteristic pseudopotential form for the interaction between the valence electrons and the ions, but modified here to incorporate the effects of the dielectric continuum. The pseudopotential $v_{pe}(q)$ used in (1b) is assumed local; note that the ion density operator is $\hat{\rho}^0(\vec{q}) = \sum_i \bar{R} e^{i\vec{q} \cdot \vec{R}}$. Term (1c) is the Coulomb energy of point charges, also in the dielectric continuum. The terms in (1d) are, respectively, the sum of all $q = 0$ terms and the screened van der Waals interactions. As is well known, E_0 has an inverse volume dependence⁶: If n_v is the mean valence electron density, it can be written as

$$E_0 = \frac{\alpha}{4\pi r_s^3/3} \left[\frac{e^2}{2a_0} \right], \quad (2)$$

where

$$r_s a_0 = (3/4\pi n_v)^{1/3}.$$

The screened fluctuating dipole interaction between ions is⁷

$$\phi_L^*(r) = \int_{-\infty}^{\infty} \frac{du}{2\pi} \alpha_0^2(iu) \left[\left(\frac{\partial^2 v(r, iu)}{\partial r^2} \right)^2 + \frac{2}{r^2} \left(\frac{\partial v(r, iu)}{\partial r} \right)^2 \right], \quad (3)$$

where

$$v(r, iu) = \int \frac{d\vec{q}}{(2\pi)^3} \left| \frac{v_{pe}(q)}{\epsilon_{eg}(q, iu)} \right| e^{i\vec{q} \cdot \vec{r}},$$

the quantity $\epsilon_{eg}(q, \omega)$ being the wave-number- and frequency-dependent dielectric function of the interacting electron gas.

Perturbation theory can be applied in a straightforward manner to (1). The contributions to the ground-state energy are then: (a) the corrected energy of the interacting electron gas, which in Ry per electron, is⁸

$$E'_{eg} = E_{eg} + E'_w, \quad (4a)$$

where

$$E_{eg} = \frac{2.21}{r_s^2} - \frac{0.916}{r_s} + E_{corr}, \quad (4b)$$

and

$$E'_w = \frac{1}{2\Omega} \sum_{\vec{q} \neq 0} S_{eg}(q) \frac{v_{pe}^2(q)}{v_c(q)} [\epsilon_c^{-1}(q) - 1], \quad (4c)$$

and where $S_{eg}(q)$ is the static structure factor of the interacting electron gas; (b) the corrected Madelung energy⁹

$$E'_M = E_M + E_{Mc}, \quad (5a)$$

where

$$E_M = - \frac{\alpha_M Z^{1/3}}{r_s}, \quad (5b)$$

$$E_{Mc} = \frac{1}{2\Omega} \sum_{\vec{q} \neq 0} Z v_c(q) S_{ion}(q) [\epsilon_c^{-1}(q) - 1], \quad (5c)$$

and S_{ion} is the ensemble averaged ionic structure

factor; (c) the corrected band-structure energy

$$E_{BS}^{(2)} = \frac{1}{2} \frac{NZ}{\Omega} \sum_{\vec{q} \neq 0} \left[\frac{v_{ps}(q)}{\epsilon_c(q)} \right]^2 \chi^0(q) S_{ion}(q) , \quad (6)$$

where $\chi^0(q)$ is the first-order polarizability of the interacting electron gas; and (d) the aggregate of all $q = 0$ terms, as given by (2). If these terms are augmented by the screened fluctuating dipole interactions, the total static lattice ground-state energy can be written

$$E(r_s) = NZ(E_{eg}' + E_M' + E_{BS}^{(2)} + E_0) + \frac{1}{2} \sum_{\vec{R}, \vec{R}'} \phi_L^{\infty}(\vec{R} - \vec{R}') . \quad (7)$$

Here the band-structure energy has been calculated to second order in the electron-ion pseudopotential. For monovalent metals (such as potassium) this neglect of higher-order band-structure energy terms is satisfactory.¹⁰ The corrections associated with $\epsilon_c(q)$ are also calculated within a linear response framework, again a reasonable approximation since the effects we are incorporating here are, in any event, fairly small.

III. ZERO-TEMPERATURE ISOTHERM

If F is the Helmholtz free energy of a system of N particles at temperature T , then the pressure is $p = -(\partial F / \partial \Omega)_{T,N}$. At $T = 0$, $F = E$, which is given by (7). The various contributions to E require the averaged core-dielectric function $\epsilon_c(q)$, the frequency-dependent valence-electron dielectric function $\epsilon(q, \omega)$, the frequency-dependent ionic polarizability $\alpha(\omega)$, and the valence-electron static response functions.

Provided the background dielectric constant $\epsilon_c(q = 0)$ is reasonably close to unity, as is the case here, we may neglect local-field corrections and write, as earlier

$$\epsilon_c(q) = 1 + 4\pi n_i \alpha(0) \quad (q \rightarrow 0) . \quad (8)$$

In the opposite limit ($q > 2\pi/d$, where d is an ionic diameter) we make a local-density approximation, taking the large wave-vector limit of the Lindhard result¹⁰

$$\epsilon_c(q) = 1 + \frac{1}{3\pi k_F^2 a_0} \left[\frac{2k_F^2}{q} \right]^4 . \quad (9)$$

Here k_F^2 is a characteristic Fermi wave vector corresponding to a locally uniform core-electron density n_c . Let $x = (q/2k_F)$; then for $Z = 1$, a simple interpolation between (8) and (9) is

$$\epsilon_c(q) = 1 + 4\pi n_i \alpha(0) \left[1 + 4 \left[\frac{n_v}{n_c} \right] \left[\frac{\alpha(0)}{a_0^3} \right] (k_F a_0)^4 x^4 \right]^{-1} , \quad (10)$$

where $\alpha(0) = \alpha(\omega = 0)$ and $k_F^3 = 3\pi^2 n_v$ (v refers to the valence electrons). This form for $\epsilon_c(q)$ is similar to the wave-vector-dependent dielectric functions used in semiconductors and other narrow-gap insulators.¹¹ It is plotted in Fig. 1 for the choice¹² $\alpha(0) = 0.9 \text{ \AA}^3$ and¹³ $n_c = 8n_v$.

To evaluate the correction to the standard electron-gas energy, we note that the second term of (4) can be identified as one-body and two-body contributions, that is,

$$E_{vv}' = \frac{1}{2\Omega} \sum_{\vec{q} \neq 0} v_{ps}^2(q) \frac{1}{v_c(q)} \left[\frac{1}{\epsilon_c(q)} - 1 \right] \quad (11)$$

$$+ \frac{1}{2\Omega} \sum_{\vec{q} \neq 0} [S_{eg}(q) - 1] v_{ps}^2(q) \frac{1}{v_c(q)} \left[\frac{1}{\epsilon_c(q)} - 1 \right] . \quad (12)$$

For an empty-core pseudopotential¹⁴ with core radius r_c and the interpolation form (10), the first of these can be evaluated in closed form and the result is (in rydbergs)

$$-(k_F a_0)(G/2a^3)[1 + e^{-\sqrt{2}\omega s}(\cos\sqrt{2}as + \sin\sqrt{2}as)] , \quad (13)$$

with

$$G = (n_c/n_v)(3k_F a_0)^{-1} ,$$

$$a^4 = G[1 + 4n_i \alpha(0)]/4\pi n_i \alpha(0) ,$$

and

$$s = 2k_F r_c .$$

To determine (12) it is sufficiently accurate to take

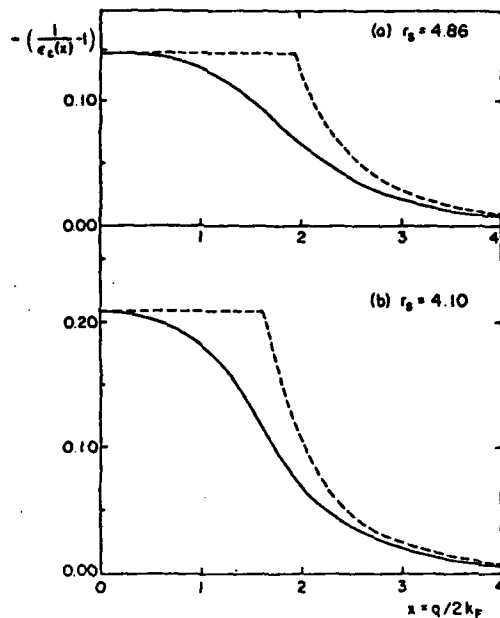


FIG. 1. Interpolated form for $\epsilon_c(q)$ for potassium. The dotted curves show the high- and low- q limits of $\epsilon_c(q)$. The solid curve is from Eq. (10). (a) $r_s = 4.86$ ($\Omega/\Omega_0 = 1.0$); (b) $r_s = 4.10$ ($\Omega/\Omega_0 = 0.6$).

the Hartree-Fock result¹⁵ for the electron-gas structure factor $S_{eg}(q)$, i.e.,

$$S_{eg}(q) = \frac{3}{2}x - \frac{1}{2}x^3 \quad (x < 1), \quad (14)$$

$$S_{eg}(q) = 1 \quad (x < 1),$$

$$\begin{aligned} \phi_L^2(R) = & -\frac{e^2}{2a_0} \frac{3\hbar\omega_0}{4(e^2/2a_0)} \frac{1}{[1 + (\omega_p/\omega_0)^2]} \left(\frac{a_0}{a_0^3} \right)^2 \left(\frac{a_0}{R} \right)^6 \\ & + \frac{\hbar\omega_p}{(e^2/2a_0)} \frac{1}{2\pi} \int dy \left(\frac{a^2(iu)}{a_0^6} \right) f_1(\vec{R}, iu) \quad \left(y = \frac{u}{\omega_p} \right), \end{aligned} \quad (17)$$

with

$$\begin{aligned} F_1(R, iu) = & [1 + (u/\omega_p)^2]^{-1} \cosh^4 Qr_c e^{-2QR} \\ & \times \left[6 \left(\frac{a_0}{R} \right)^6 + 12Qa_0 \left(\frac{a_0}{R} \right)^5 + 10(Qa_0)^2 \left(\frac{a_0}{R} \right)^4 + 4(Qa_0)^3 \left(\frac{a_0}{R} \right)^3 + (Qa_0)^4 \left(\frac{a_0}{R} \right)^2 \right]. \end{aligned}$$

Here the quantity Q is defined by

$$Q^2 = k_{TF}^2 [1 + (u/\omega_p)^2].$$

The sum in (17) can be evaluated with relatively little computational effort. Finally, we determine the parameter α in E_0 by the zero-pressure condition⁶

where

$$x = q/2k_F.$$

Since $\epsilon_c(x)$ is already close to unity, it is reasonable to ignore further corrections to the correlation energy arising from the modification of the effective electron-electron interaction because of core-polarization effects.

We turn now to the energy of the screened van der Waals interactions: Its determination requires the frequency-dependent atomic and electron-gas polarizabilities. Again, since this contribution is not a major one, we may make reasonable approximations in both quantities. For the atomic polarizability we take the usual Lorentz form

$$\alpha(\omega) = \alpha(0)[1 - (\omega/\omega_0)^2]^{-1}, \quad (15)$$

where ω_0 is a characteristic frequency (estimated to be the equivalent of 47 eV for potassium¹⁶). The wave-vector- and frequency-dependent dielectric function for the valence electrons is taken to have the simple form¹⁷

$$\epsilon(q, \omega) = 1 + k_{TF}^2/(q^2 - k_{TF}^2\omega^2/\omega_p^2), \quad (16)$$

where k_{TF} is the Thomas-Fermi wave vector. Notice that this leads to the familiar $q \rightarrow 0$ (for $\omega = 0$) and $\omega \rightarrow 0$ (for $q = 0$) limits. The point is that the use of (15) and (16) in conjunction with (3) gives

$$NZE_{vdW} = \frac{1}{2} \sum_{R \neq 0} \phi_L^2(\vec{R}),$$

where

which leads to

$$\alpha = \frac{4\pi}{9} \left[r_{s0} (0.916 + Z^{2/3} \alpha_M) + 0.031 r_{s0} - r_{s0}^2 \left(\frac{\partial E'}{\partial r_s} \right)_{r_{s0}} - 4.42 r_{s0} \right], \quad (18)$$

where E' refers to the sum of the energy contributions other than those having their origin in electron-gas and electrostatic terms. In the case of potassium the zero-pressure electron spacing parameter¹⁸ is $r_{s0} = 4.860$.

The total energy of bcc potassium can now be obtained by adding the contributions given by Eqs. (4)–(6) and (17) with α chosen to give the correct zero-pressure density, and subsequently held fixed. The various contributions to the energy and pressure are listed in Table I for a sequence of volume compressions. The $T = 0$ equation of state is shown in Fig. 2 and compared there with the low-temperature experimental results of Monfort and Swenson.¹⁹ Above 20 kbar the comparison is made to an extrapolation achieved using¹⁹

$$P_{T=0}(\Omega) = 37.0[(\Omega_0/\Omega)^{3.85} - 1]/3.85 \quad (19)$$

in units of kbar. It is clear from Fig. 2 that the agreement between theory and experiment is satisfactory.

The importance of core-polarization contributions can be judged by comparing these results with core effects neglected altogether. In practice this is (unintentionally) carried out by the fitting procedure in which all $q = 0$ terms are assumed incorporated in the aggregate E_0 . Since the actual zero pressure density is determined by *all* contributions to the energy, the explicit neglect of core polarization is equivalent to assuming their implicit incorporation in E_0 (and assigning them thereby an inverse

volume dependence). Figure 3 and Table II summarize the results of such a procedure. A direct comparison of these two sets of results show that though there is a qualitative similarity (and quantitative to within 30%) the effects of core polarization are not small in potassium. The comparison also shows that to the extent that the difference in energies computed by the two different methods can be assumed inversely volume dependent, much of the difference can be absorbed in E_0 .

IV. DISCUSSION

As might have been anticipated from the fact that the potassium ion is quite polarizable, we find that core-polarization effects in postassium metal contribute noticeably to its thermodynamic functions, particularly at high pressures. We now examine the degree to which this conclusion may depend on the approximations and numerical procedures adopted. First, the interpolation form used for $\epsilon_c(q)$ is plausible on physical grounds, is convenient for numerical reasons, but is nevertheless still approximate. On the other hand, much of the contribution from these terms originates with the small- q contribution where the background dielectric constant is best known. In the same long-wavelength limit the dipole approximation used throughout is expected to be valid and so is the standard procedure for evaluating local-field effects.²⁰ When wavelengths become comparable to the spatial extent of the core-electron

TABLE I. Computed energy and pressure for potassium as a function of volume with core-polarization effects taken into account. The various quantities are defined in the text. Ω_0 is the zero-pressure volume.

Ω/Ω_0	Energy (Ry/electron)							
	E_{eg}	E_M	E_0	E_{Mc}	E_{BS}	E'_{ew}	E_{vdW}	E_{tot}
1.0	-0.1610	-0.3687	0.2793	-0.1003	-0.0149	-0.0557	-0.0012	-0.4225
0.9	-0.1620	-0.3819	0.3104	-0.1085	-0.0171	-0.0609	-0.0015	-0.4215
0.8	-0.1628	-0.3972	0.3492	-0.1184	-0.0199	-0.0673	-0.0019	-0.4183
0.7	-0.1633	-0.4152	0.3991	-0.1302	-0.0237	-0.0751	-0.0024	-0.4108
0.6	-0.1633	-0.4371	0.4656	-1448	-0.0287	-0.0852	-0.0032	-0.3967
Pressure (kbar)								
Ω/Ω_0	$P(E_{eg} + E_M + E_0)$	$P(E_{vdW})$	$P(E_{Mc})$	$P(E_{BS})$	$P(E'_{ew})$	P_{tot}	P_{exp}^a	
	44.6	-0.7	-23.3	-6.0	-14.5	0.0	0.0	
0.9	59.3	-1.0	-27.5	-7.6	-17.5	5.7	4.8	
0.8	80.7	-1.3	-32.8	-9.9	-21.5	15.3	13.1	
0.7	113.0	-2.0	-40.0	-13.1	-27.0	30.9	(28.3)	
0.6	164.5	-3.0	-49.8	-18.1	-35.2	58.5	(59.1)	

^aReference 19. Numbers in parentheses are obtained by extrapolation.

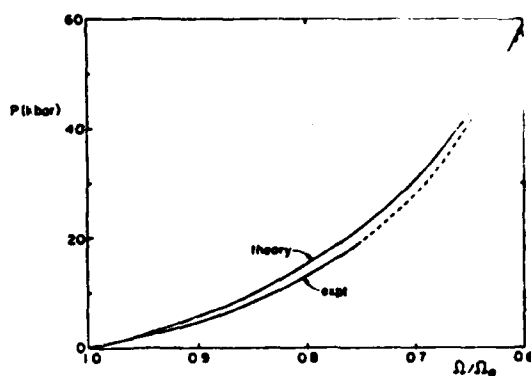


FIG. 2. Comparison of computed equation of state of potassium (core-polarization effects included) with the experimentally determined function. The dotted portion of the experimental curve is obtained by extrapolation of Eq. (32) (Ref. 19).

charge distribution, however, the description in terms of translationally invariant core-electron response functions is not strictly justified. For such wavelengths it is the case that the dielectric function approaches unity quite closely so that though the interpolation form we use [Eq. (10)] lacks the expected symmetry, the error thereby introduced is certainly small.

It is also worth noting that the parameters $\alpha(0)$ and

ω_0 can be expected to be weak functions of density.²¹ Furthermore, it is well known that a nonlocal pseudopotential is required for a correct description of band structure of potassium (there are empty d -symmetry bands lying above the Fermi energy^{22,23}). Of the terms most affected by such considerations, the band-structure energy is foremost. Nevertheless, once such nonlocal contributions are averaged, as in the construction of the total energy, the resulting uncertainties in the equation of state are not great. The reason is that the contributions to the equation of state from E_{BS} are -6 kbar at $\Omega/\Omega_0 = 1$, and -18 kbar at $\Omega/\Omega_0 = -0.6$. If E_{BS} were completely omitted, then at $p = 0$, E_0 would acquire (by virtue of the fitting procedure) an additional term to cancel the -6 kbar. Since E_0 is assigned an inverse volume dependence, it would yield -17 kbar at $\Omega/\Omega_0 = 0.6$, thus leading to a total error of only 1 kbar. At very high pressures, the d bands which are the major source of this nonlocality, might actually intersect the Fermi surface, a phenomenon observed²⁴ in Cs at around 42.5 kbar. The nearly-free-electron approach, on which our calculations have been based, will then be invalidated. We note that in the experimentally determined equation of state (at room temperature) no such transition of this nature has so far been observed for pressure up to 50 kbar.^{19,25} All of these effects may need ult-

TABLE II. Computed energy and pressure for potassium as a function of volume (core polarization effects neglected).

Ω/Ω_0	Energy (Ry/electron)		$E_{BS}^{(2)}$	E_{tot}
	$E_{eg} + E_M + E_0$			
1.0	-0.3702		-0.0166	-0.3868
0.9	-0.3667		-0.0195	-0.3862
0.8	-0.3607		-0.0233	-0.3840
0.7	-0.3507		-0.0283	-0.3790
0.6	-0.3346		-0.0348	-0.3694

Ω/Ω_0	Pressure (kbar)		P_{tot}	$P_{exp.}$
	$P(E_{eg} + E_M + E_0)$	$P(E_{BS}^{(2)})$		
1.0	7.9	-7.9	0.0	0.0
0.9	14.1	-10.2	3.9	4.8
0.8	23.4	-13.3	10.2	13.1
0.7	38.2	-17.4	20.8	(28.3)
0.6	62.7	-22.8	39.9	(59.1)

*Reference 19. Numbers in parentheses are obtained by extrapolation.

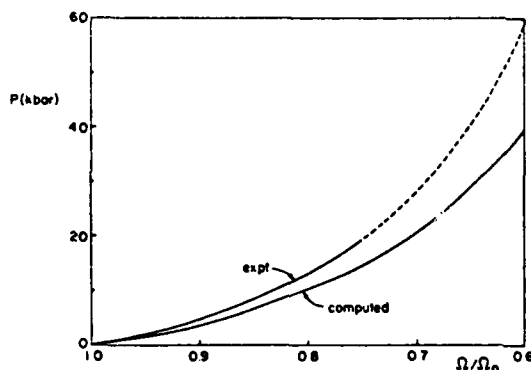


FIG. 3. The computed equation of state shown in this figure neglects core effects.

mately further consideration, but within a few kbar will not alter the principal conclusion, namely that at high pressure core-polarization effects in potassium appreciably modify its equation of state.

ACKNOWLEDGMENTS

This work has been supported by the Army Research Office, Durham, North Carolina, under Grant No. DAAG-29-79-C-0188.

*Present address: Bell Laboratories, Holmdel, New Jersey.

¹K. K. Mon, N. W. Ashcroft, and G. V. Chester, Phys. Rev. B 19, 5103 (1979).

²C. A. Kukkonen and J. W. Wilkins, Phys. Rev. B 19, 6075 (1979); C. A. Kukkonen, Ph.D. thesis, Cornell University, 1975 (unpublished).

³J. Cheung and N. W. Ashcroft, Phys. Rev. B 23, 2484 (1981).

⁴T. Soma, J. Phys. F 10, 1401 (1980).

⁵Such thermal contributions to the equation of state can be estimated from the Mie-Grüneisen equation of state. In the alkali metals these can be a few kbar (see Ref. 4).

⁶N. W. Ashcroft and D. C. Langreth, Phys. Rev. 155, 682 (1967).

⁷J. J. Rehr, E. Zaremba, and W. Kohn, Phys. Rev. B 12, 2062 (1975); J. Mahanty and R. Taylor, *ibid.* 17, 554 (1978).

⁸In (4b), E_{corr} is the correlation energy of the interacting electron gas for which we take the Nozières-Pines form [D. Pines and P. Nozières, *The Theory of Quantum Liquids* (Benjamin, N.Y., 1966)]. Other forms lead to very similar results; see, for example, P. Vashista and K. S. Singwi, Phys. Rev. B 6, 875 (1972). In (4c), $v_p(q)$ is a pseudopotential approximating the coupling of valence electrons to fluctuating dipoles, as discussed in Refs. 1 and 3.

⁹In (5b), α_M is the standard Madelung constant; see D. C. Wallace, *Thermodynamics of Crystals* (Wiley, N.Y., 1972); C. Friedli and N. W. Ashcroft, Phys. Rev. B 12, 5552 (1975).

¹⁰See, for example, Ref. 4 and M. L. Cohen and V. Heine, in *Solid State Physics*, edited by H. Ehrenreich, F. Seitz, and D. Turnbull (Academic, New York, 1970), Vol. 24, p. 38.

¹¹D. R. Penn, Phys. Rev. 128, 2093 (1962); W. Brandt and J. Reinheimer, Can. J. Phys. 46, 607 (1968); G. Srinivasan, Phys. Rev. 178, 1244 (1969).

¹²A. Dalgarno, Adv. Phys. 11, 281 (1962).

¹³Here we are estimating the local density appropriate to the $3s^23p^6$ shell of the potassium ion, ignoring contributions from the far less polarizable inner shell.

¹⁴N. W. Ashcroft, Phys. Lett. 23, 48 (1966); N. W. Ashcroft, J. Phys. C 1, 232 (1968).

¹⁵The use of (14) in $(1/2\Omega) \sum_{q \neq 0} v_p(q) [S_{\text{ex}}(q) - 1]$ gives only the exchange energy.

¹⁶N. W. Ashcroft and N. D. Mermin, *Solid State Physics* (Holt, Rinehart and Winston, New York, 1976).

¹⁷As noted by Rehr *et al.* (Ref. 7), this form, though approximate, nevertheless yields approximately 90% of the energy bound up in the screened fluctuating dipole interactions. In (16), $\omega_p = (4\pi n_e e^2/m)^{1/2}$ is the plasma frequency and k_{TF} is the Thomas-Fermi wave vector, $k_{TF}^2/k_F^2 = (16/3^2)^{2/3} r^4$.

¹⁸C. S. Barrett, Acta Cryst. 9, 671 (1956); D. R. Schouten and C. A. Swenson, Phys. Rev. B 10, 2175 (1974).

¹⁹C. E. Monfort, III, and C. A. Swenson, J. Phys. Chem. Solids 26, 291 (1965).

²⁰S. L. Adler, Phys. Rev. 126, 413 (1962); S. R. Nagel and T. A. Witten, Jr., Phys. Rev. B 11, 1623 (1975).

²¹They are also related by a sum rule: See J. M. Ziman, *Principles of the Theory of Solids*, 2nd ed. (Cambridge University Press, London, 1972).

²²M. J. G. Lee and L. M. Falicov, Proc. R. Soc. London, Sect. A 304, 319 (1968).

²³J. Moriarty, Phys. Rev. B 5, 2006 (1972); 6, 4445 (1972); 10, 3075 (1974).

²⁴A. Jayaraman, R. C. Newton, and J. M. McDonough, Phys. Rev. 159, 527 (1967); D. B. McWhan, G. Parisis, and D. Bloch, J. Phys. F 4, L69 (1974).

²⁵S. N. Vaidya, I. C. Getting, and G. C. Kennedy, J. Phys. Chem. Solids 32, 2545 (1971); F. P. Bundy and H. M. Strong, in *Solid State Physics*, edited by H. Ehrenreich, F. Seitz, and D. Turnbull (Academic, New York, 1962), Vol. 13, p. 81.

